National Analytical Management Program (NAMP)
U.S. Department of Energy Carlsbad Field Office

Radiochemistry Webinars

Actinide Chemistry Series

- *Environmental Chemistry of Uranium and Plutonium*

Idaho National Laboratory

URS

In Cooperation with our University Partners

Oregon State University

Illinois Institute of Technology

The University of Iowa

Clemson University

1914 2014 Centennial Celebration, The University of Texas at El Paso

New Mexico State University Carlsbad

UNLV

University of California · Irvine

Meet the Presenter…

Brian Powell

Dr. Brian Powell has extensive expertise with the mobility of radionuclides in soil and groundwater systems through his research in the Department of Environmental Engineering and Earth Sciences at Clemson University, as well as previous work at the Lawrence Livermore National Laboratory and the Lawrence Berkeley National Laboratory. He has a B.S. in Chemistry from the University of Montevallo, and an M.S. and Ph.D. in Environmental Engineering and Science from Clemson University. He holds memberships in the Association of Environmental Engineering and Science Professors, the American Geophysical Union, Sigma Xi, and the American Chemical Society.
At Clemson University, Dr. Powell teaches courses in Actinide Environmental Chemistry, Environmental Radiation Protection (Lecture and Laboratory courses), Introductory Health Physics, Geochemistry, and Geochemical Reaction Modeling. Dr. Powell's major research interest is to understand interrelated chemical, biological, and physical processes that control the fate and transport of radionuclides and trace metals in the environment. These processes include sorption by minerals, interactions with nano-colloids, complexation by organic ligands, and interactions with microorganisms. He has published over 20 refereed journal publications, 16 research reports, and made nearly 50 technical presentations on these topical areas. He has conducted sponsored research dealing with topics such as nuclear forensics, evaluation of nanoparticle behavior, sorption and environmental transport of plutonium, development of radiation detection and radiation laboratory courses, evaluation of radionuclide geochemistry in wetland and subsurface sediments, solid waste performance assessments at the Savannah River Site, measurement of thermodynamic parameters supporting advanced nuclear fuel cycle chemistry, and related topics. These projects have garnered over $5M in research awards. The knowledge gained from this work can be used to evaluate risk posed by subsurface contamination, to design remediation strategies for contaminated sites, and to facilitate the use of safe disposal practices.

Contact: (864)656-1004
Email: BPOWELL@clemson.edu

CLEMSON UNIVERSITY

Part 2: Uranium Environmental Behavior

Dr. Brian A. Powell
Environmental Engineering and Earth Sciences
Clemson University

National Analytical Management Program (NAMP)
U.S. Department of Energy Carlsbad Field Office

TRAINING AND EDUCATION SUBCOMMITTEE

Outline

- Introduction: Brief overview of some sites
- Aqueous speciation in natural waters
  - Complexation with inorganic and organic ligands
  - Redox reactions
- Sorption to minerals and sediments
  - Evaluation of sorption models (empirical K_d approaches, simple SCM, bond valence based SCM)
- Precipitation/formation of nanoparticulates
- Interaction with microorganisms
- Case study: Uranium Bioremediation

Introduction – U-contaminated Sites

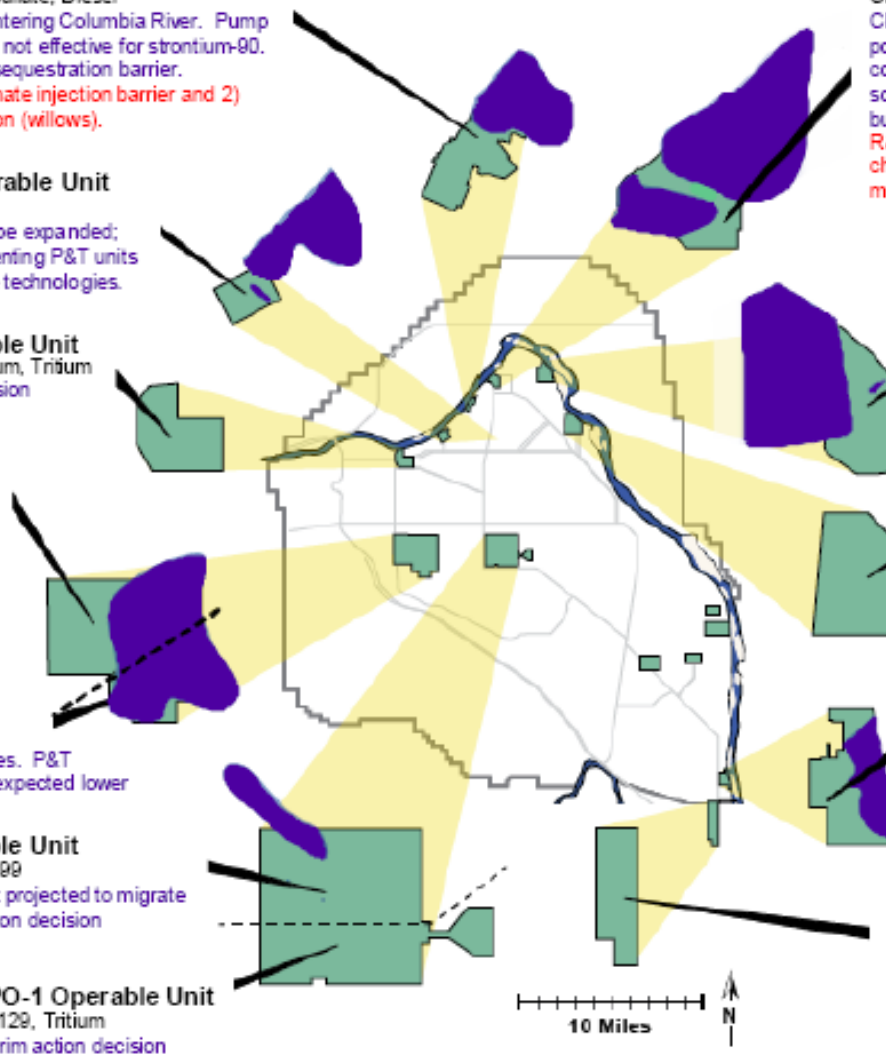

100-NR-2 Operable Unit
Strontium-90, Sulfate, Diesel
Strontium-90 entering Columbia River. Pump and treat (P&T) not effective for strontium-90. Testing in-situ sequestration barrier.
R&D: 1) phosphate injection barrier and 2) phytoremediation (willows).

100-KR-4 Operable Unit
Chromium
P&T effective, will be expanded; considering augmenting P&T units with more effective technologies.

100-BC-5 Operable Unit
Strontium-90, Chromium, Tritium
No interim action decision requiring remediation.

200-ZP-1 Operable Unit
Carbon Tetrachloride
P&T/vapor extraction providing partial containment of highest contaminant concentrations. ROD for expanded operations expected by 2009.
R&D: methods to predict plume movement and contaminant degradation.

200-UP-1 Operable Unit
Uranium, Technetium-99
P&T met interim remediation objectives. P&T operations will be continued to meet expected lower uranium requirements of final ROD.

200-BP-5 Operable Unit
Uranium, Technetium-99
Plume growing but not projected to migrate offsite. No interim action decision requiring remediation.

200-PO-1 Operable Unit
Iodine-129, Tritium
No interim action decision requiring remediation.

100-HR-3-D Operable Unit
Chromium
Chromium entering Columbia River. In northern portion of plume P&T effective in removing contaminants and controlling migration. In southern portion of plume in situ barrier effective but requires augmentations.
R&D: 1) resin system implementation and 2) chromium reduction (addition of molasses/vegetable oil).

100-HR-3-H Operable Unit
Chromium
Ongoing P&T effective in controlling plume migration and removing contaminants.

100-FR-3 Operable Unit
Strontium-90, Chromium, Nitrate, TCE
No interim action decision requiring remediation.

300-FF-5 Operable Unit
Uranium, TCE, cis-1,2-DCE
Uranium entering Columbia River, natural attenuation not meeting remediation goals; testing sequestration technologies.
R&D: polyphosphate addition to bind uranium.

1100-EM-1 Operable Unit
Trichloroethylene (TCE)
Operable Unit removed from the NPL.

http://www.em.doe.gov/pdfs/Groundwater_Booklet-2008.pdf

Introduction – U-contaminated Sites

S-3 Waste Disposal Ponds at the U.S. DOE Oak Ridge Reservation

http://public.ornl.gov/orifc/images/S3_ponds.jpg
http://public.ornl.gov/orifc/images/S3_ponds_parking_lot.jpg

Need for Understanding U and Pu Geochemistry – Risk Evaluation

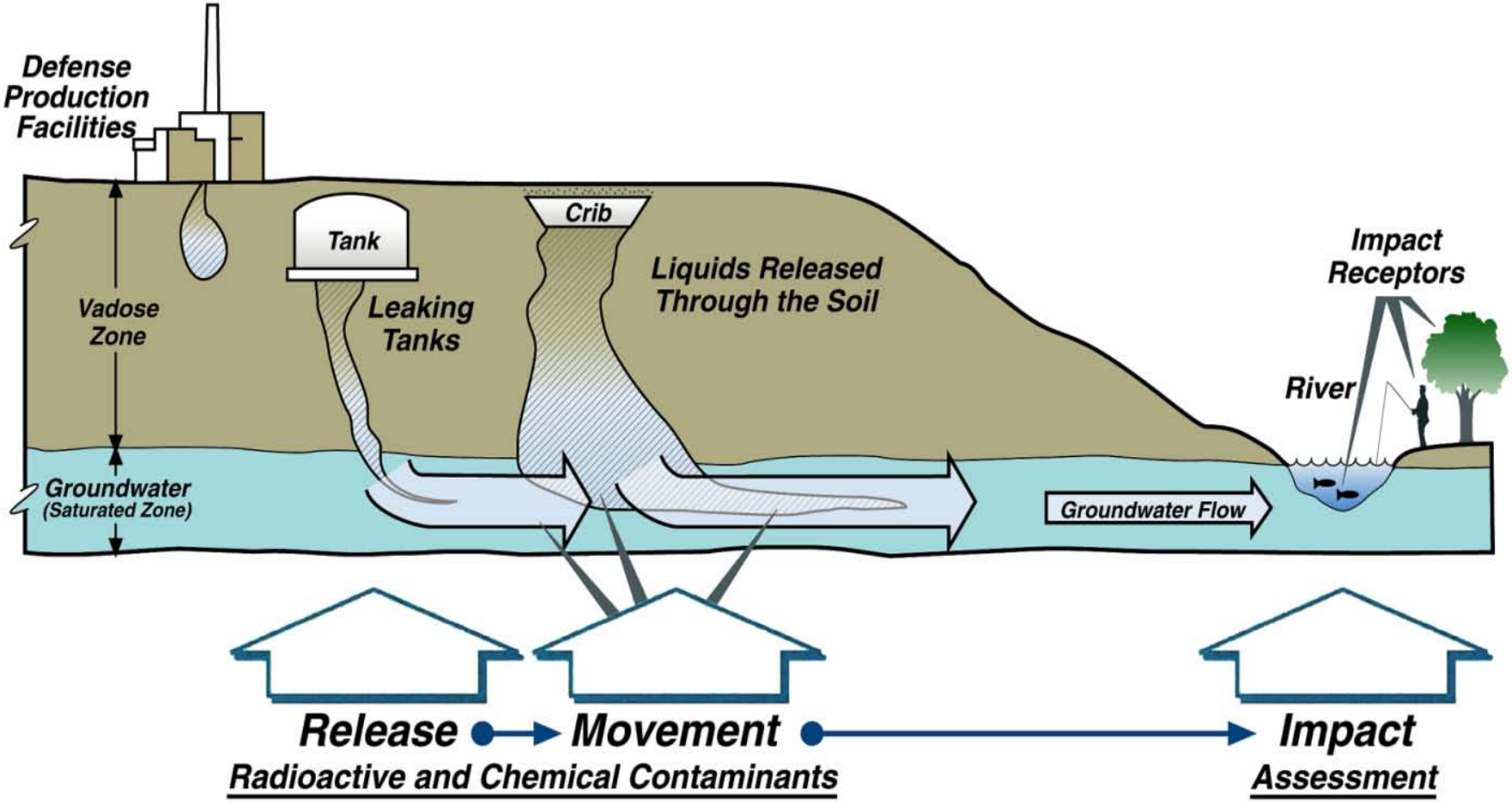

http://picturethis.pnl.gov

Major Reactions Influencing Uranium Environmental Behavior

- Aqueous Complexation

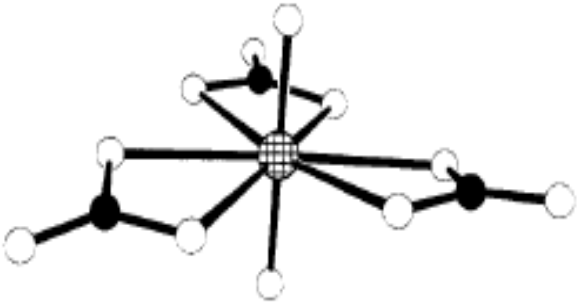

Soluble $UO_2(CO_3)_3^{4-}$ complex. Clark et al., *Chem. Rev.*, 1995, 95 (1), 25-48

- Precipitation/Dissolution

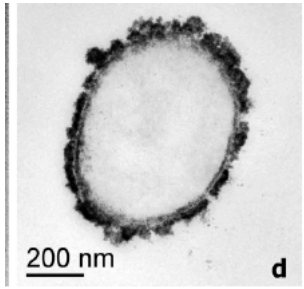

Biogenic uraninite nanoparticles, Burgos et al., 2008

- Oxidation/Reduction

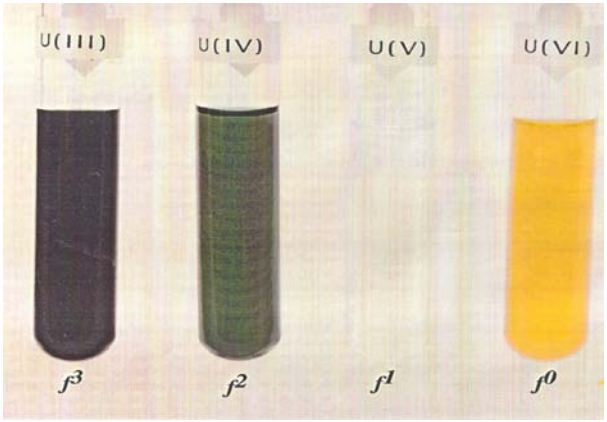

- Sorption/Desorption

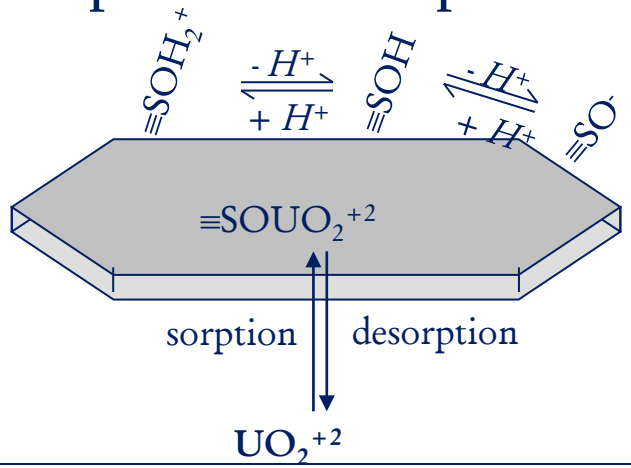

Aqueous Complexation - Outline

- Common oxidation states
- Common groundwater ions
- Hydration of the actinides
- Hydrolysis reactions
- Complexation with halides
- Complexation with oxyanions
- Complexation with natural organic matter

Equilibrium Constants

- Given reaction:

  $aA + bB \Leftrightarrow cC + dD$

- K^o is the equilibrium expression under standard conditions

- K^c is a concentration-based equilibrium constant based on the given solutions conditions

$$K^o = \frac{\{C\}^c \{D\}^d}{\{A\}^a \{B\}^b}$$

$$K^o = \frac{[C]^c \gamma_c^c [D]^d \gamma_d^d}{[A]^a \gamma_a^a [B]^b \gamma_b^b}$$

$$K^o = \frac{[C]^c [D]^d}{[A]^a [B]^b} \frac{\gamma_c^c \gamma_d^d}{\gamma_a^a \gamma_b^b}$$

$$K^o = K^c \frac{\gamma_c^c \gamma_d^d}{\gamma_a^a \gamma_b^b}$$

Different names for the same thing (products over reactants)
Stability constant = equilibrium constant = equilibrium for a metal-complex
Dissociation constant = acid/base dissociation (i.e., pK_a)
Hydrolysis constant = metal ion hydrolysis (i.e., reaction with water/OH^-)

Uranium Oxidation States

- Under environmental conditions, U(IV) and U(VI) are expected to be stable
- Similar to Pu, the tetravalent U(IV) state is relatively insoluble and immobile, while hexavalent U(VI) is more soluble and mobile in many environmental systems
- The varying mobility of Pu and U oxidation states gives rise to many redox-based remediation strategies

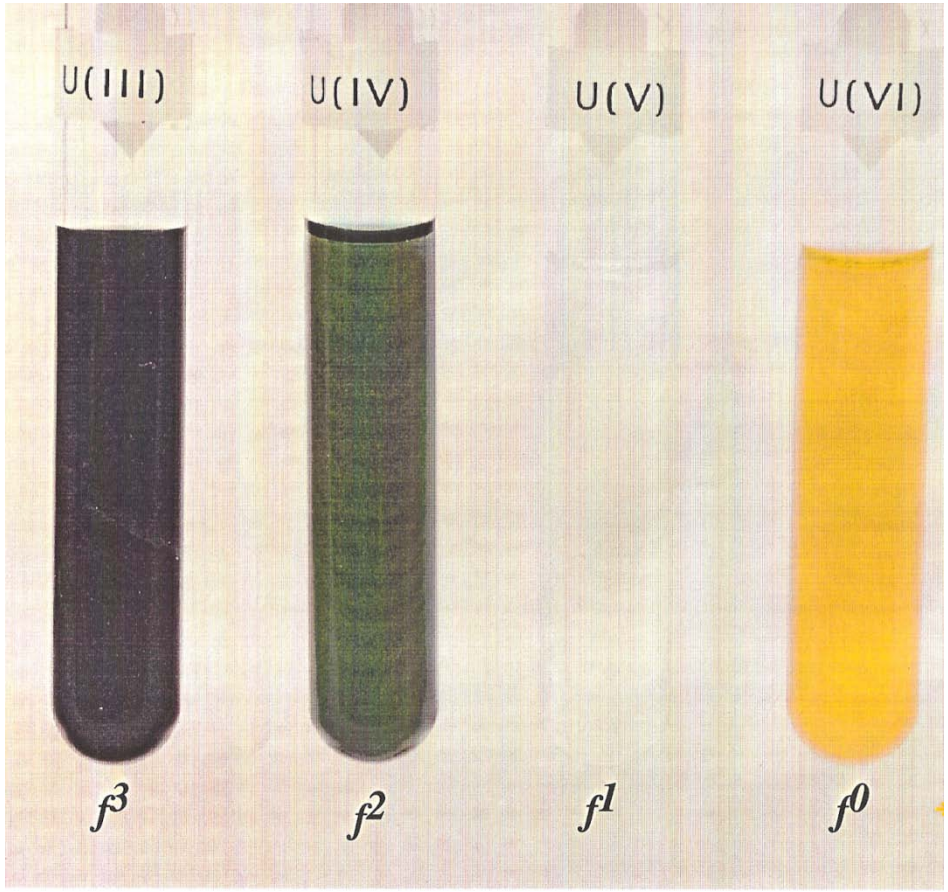

Influence of Effective Charge

- Most processes concerned with actinides in oxidation states III-VI
  - An(III) and An(IV) present as free ions
  - An(V) and An(VI) present as actinyl ions AnO_2^+ and AnO_2^{2+}
- Overall effective charge of the ions does not follow formal charge (Rao and Choppin, 1984)

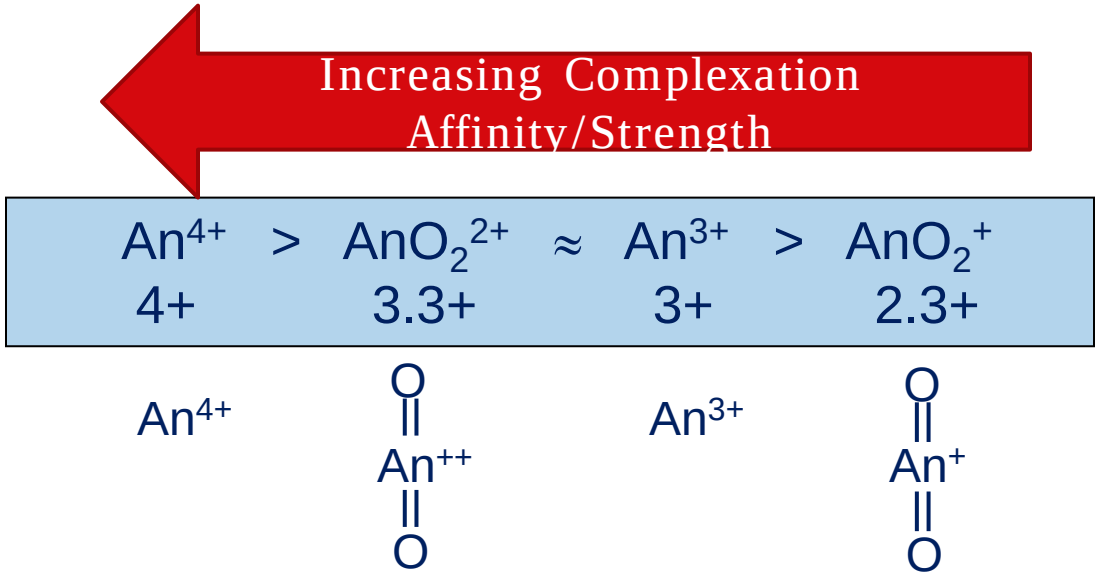

General Solution Chemistry Trends

- In neutral pH (5-9) natural waters, actinide ions hydrolysis readily. Therefore, solubility is generally limited to <10^-6 M, with the notable exception of pentavalent actinides
- Hydrolysis leads to $An(OH)_4(s)$ and $AnO_2(s)$, which may have a colloidal character
- Other dissolved heavy elements are present at solubility concentrations of the actinides. Therefore, there is significant competition for chemical reactions
- Complexing ions such as carbonate, phosphate, humic substances, etc., may stabilize actinides as monomeric ions
- All the above reactions are highly dependent on the oxidation state of the actinide
- Stability of oxidation states vary for each actinide and the components within natural waters. Redox chemistry between actinides is not necessarily comparable. However…
- Chemical behavior between oxidation states is generally similar

Actinide Hydration – $An(H_2O)_x$

- Complexation reactions with water
- f-element salts are fairly soluble in water
- Strong ion-dipole interactions create a primary hydration sphere
- Additional hydration layers created from additional dipole-dipole interactions
- Hydration state and number is influenced by effective charge (see next slide)

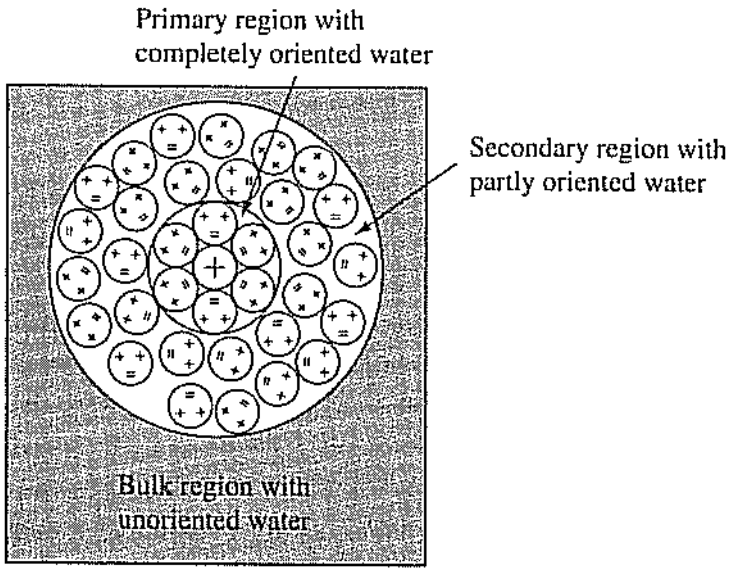

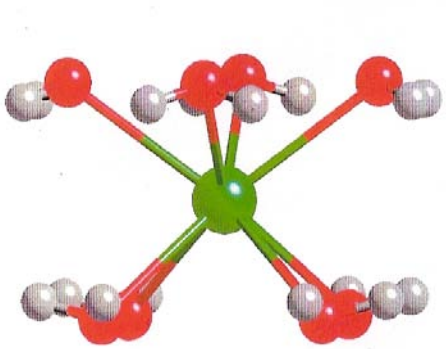

An(IV), $N_{H2O} = 8$

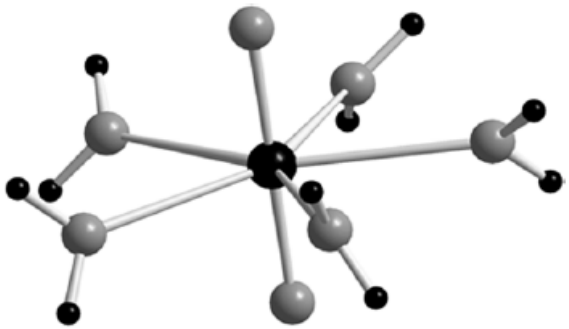

An(VI), $N_{H2O} = 5$
Vallet et al., 2001

Actinide Hydration

- U(III) - data indicate 9-10 hydrating waters with a U-O coordination number of 9 or 10
- U(IV) – 8 hydrating waters with an U-O coordination number of 8
- U(V) – 5 coordinating waters with an overall U-O coordination number of 7 (5 waters and 2 axial oxygen atoms)
- U(VI) – 5 or 6 coordinating waters with an overall U-O coordination number of 7 or 8 (5 or 6 waters with 2 axial oxygen atoms)

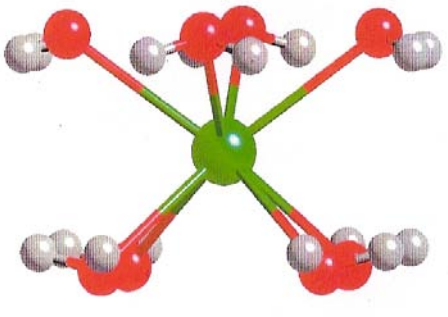

An(IV), N_{H2O} = 8

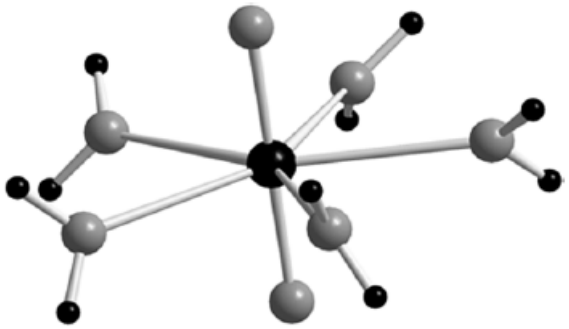

An(VI), N_{H2O} = 5

Vallet et al., 2001

Actinide Hydrolysis

- General reaction

$$xAn^{z+} + yH_2O \Leftrightarrow An_x(OH)_y^{xz-y} + yH^+$$

$$\beta^o = \frac{\{An_x(OH)_y^{xz-y}\}\{H^+\}^y}{\{An^{z+}\}^x\{H_2O\}^y}$$

- Occurs for all actinide ions
  - An(IV) – begins in acidic (~pH 1) solutions
  - An(III), An(VI) – begins in weakly acidic to neutral solutions
  - An(V) – begins above pH 8

- Note: reaction can be written as

$$xAn^{z+} + yOH^- \Leftrightarrow An_x(OH)_y^{xz-y}$$

$$\beta^{o*} = \frac{\{An_x(OH)_y^{xz-y}\}}{\{An^{z+}\}^x\{OH^-\}^y}$$

- What is the relationship between b^o and b^{o*}?

- What trend do you expect regarding the strength of hydrolysis from An(III), An(IV), An(V), An(VI)?

Tetravalent Actinide Hydrolysis

Chemistry of the Actinide and Transactinide Elements, 2006

Table 23.11 *Hydroxide complexation constants for An(IV) cations, $I = 0$ M (Neck and Kim, 2001).*

	Th(IV)	*U(IV)*	*Np(IV)*	*Pu(IV)*
$\log K^{o}_{sp(cr)}$	-54.2 ± 1.3	-60.86 ± 0.36	-63.7 ± 1.8	-64.0 ± 1.2
$\log K^{o}_{sp(am)}$	-47.0 ± 0.8	-54.5 ± 1.0	-56.7 ± 0.4	-58.5 ± 0.7
$\log \beta^{o}_{11}$	11.8 ± 0.2	13.6 ± 0.2	14.5 ± 0.2	14.6 ± 0.2
$\log \beta^{o}_{12}$	22.0 ± 0.6	26.9 ± 1	28.3 ± 0.3	28.6 ± 0.3
$\log \beta^{o}_{13}$	31.0 ± 1.0	37.3 ± 1	39.2 ± 1	39.7 ± 0.4
$\log \beta^{o}_{14}$	38.5 ± 1.0	46.0 ± 1.4	47.7 ± 1.1	48.1 ± 0.9
$\log \beta^{o}_{24}$	59.1[a]	–	–	–
$\log \beta^{o}_{4,12}$	141.3	–	–	–
$\log \beta^{o}_{6,15}$	176.0	196[b]	–	–

[a] Calculated for $I = 0$ from data in Moon (1989).
[b] $\log \beta_{6,15}$ for $I = 3$ M $NaClO_4$ (Baes and Mesmer, 1976).

Constants for rxn: $An^{4+} + xOH^{-} \Leftrightarrow An(OH)_x^{4-x}$

U(IV) Hydrolysis

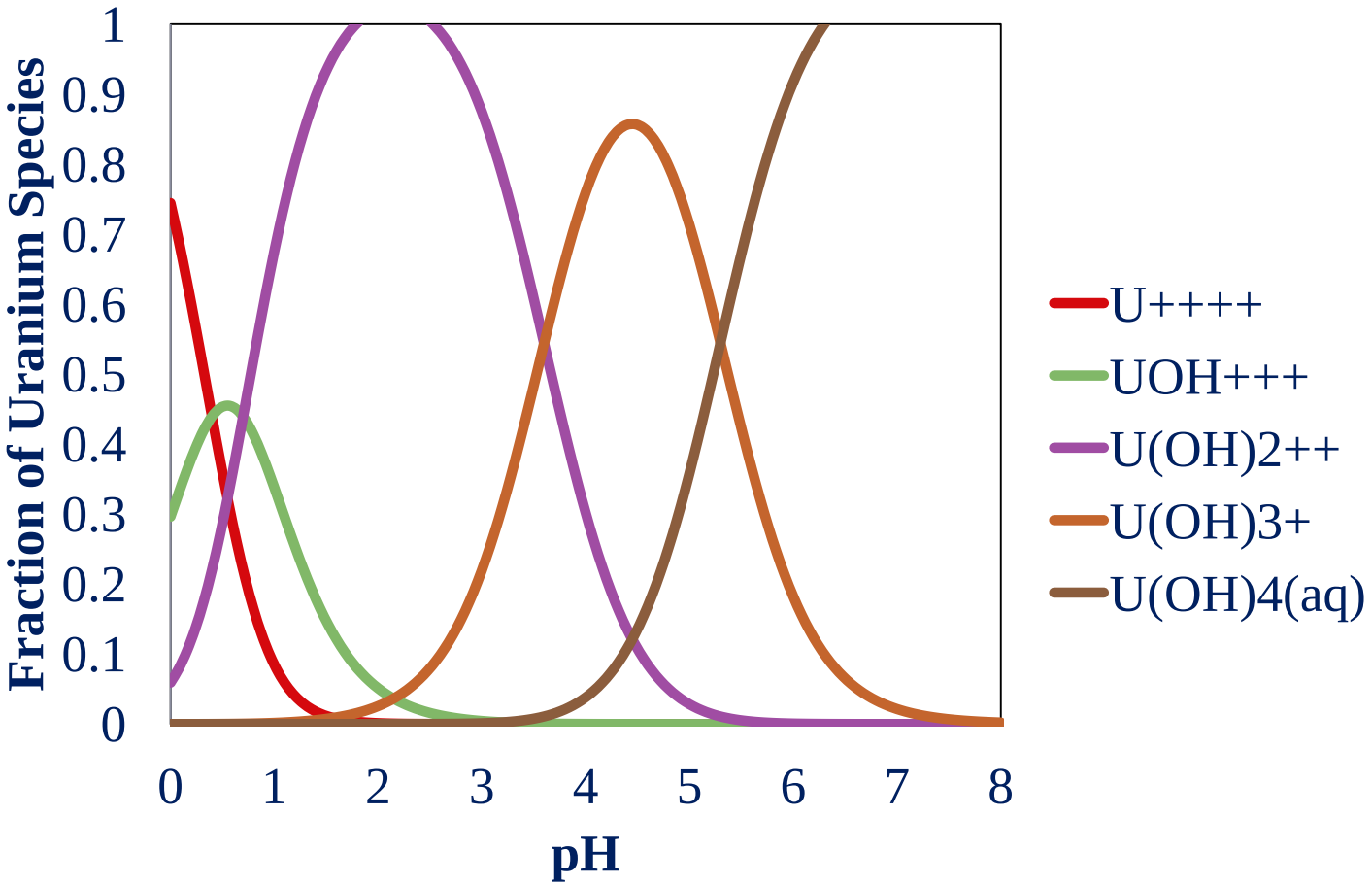

- System conditions: [U(VI)] = 10nM, ionic strength = 10mM, variable pH
- Modeled with hydrolysis constants from previous slide using Hyss

U(VI) Hydrolysis, UO_2^{2+}

- Hydrolysis of U(VI) has been extensively studied
- Hexavalent actinides form a wide variety of polynuclear species

Table 5.33 *Stoichiometry and stability constants for the hydrolysis complexes of uranium. The stability constants refer to zero ionic strength and a temperature of* 25°C*; data from Grenthe* et al. (1992), *Guillaumont* et al. (2003), *and Baes and Mesmer* (1976).

Uranium(VI) Chemical reaction	$log^*\beta_{p,q}$
$UO_2^{2+} + H_2O \rightleftharpoons UO_2OH^+ + H^+$	–5.25
$UO_2^{2+} + 2H_2O \rightleftharpoons UO_2(OH)_2(aq) + 2H^+$	–12.15
$UO_2^{2+} + 3H_2O \rightleftharpoons UO_2(OH)_3^- + 3H^+$	–20.25
$UO_2^{2+} + 4H_2O \rightleftharpoons UO2(OH)_4^{2-} + 4H^+$	–32.40
$2UO_2^{2+} + H_2O \rightleftharpoons (UO_2)_2OH^{3+} + H^+$	–2.7
$2UO_2^{2+} + 2H_2O \rightleftharpoons (UO_2)_2(OH)^{2+} + 2H^+$	–5.62
$3UO_2^{2+} + 5H_2O \rightleftharpoons (UO_2)_3(OH)_5^+ + 5H^+$	–15.55
$3UO_2^{2+} + 7H_2O \rightleftharpoons (UO_2)_3(OH)_7^+ + 7H^+$	–32.7
$4UO_2^{2+} + 7H_2O \rightleftharpoons (UO_2)_4(OH)_7^+ + 7H$	–21.9

[a] Estimates from Baes and Mesmer (1976).

The Chemistry of the Actinide and Transactinide Elements, 2006

Uranium Hydrolysis, $[UO_2^{2+}]$ = 1E-8 mol/L

Modeled using Geochemist Workbench, LLNL Database

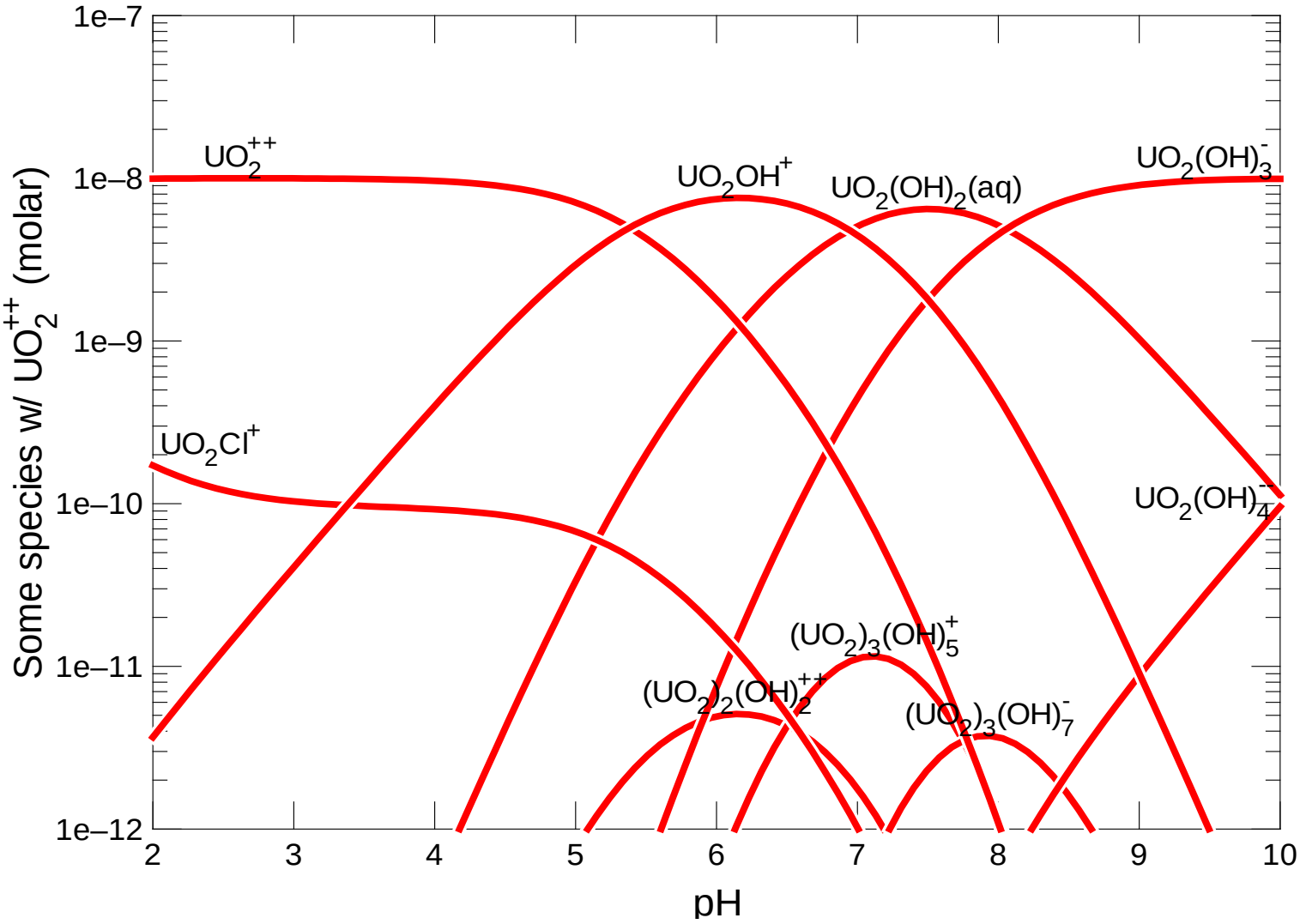

Uranium Hydrolysis, $[UO_2^{2+}]$ = 1E-3 mol/L

Modeled using Geochemist Workbench, LLNL Database

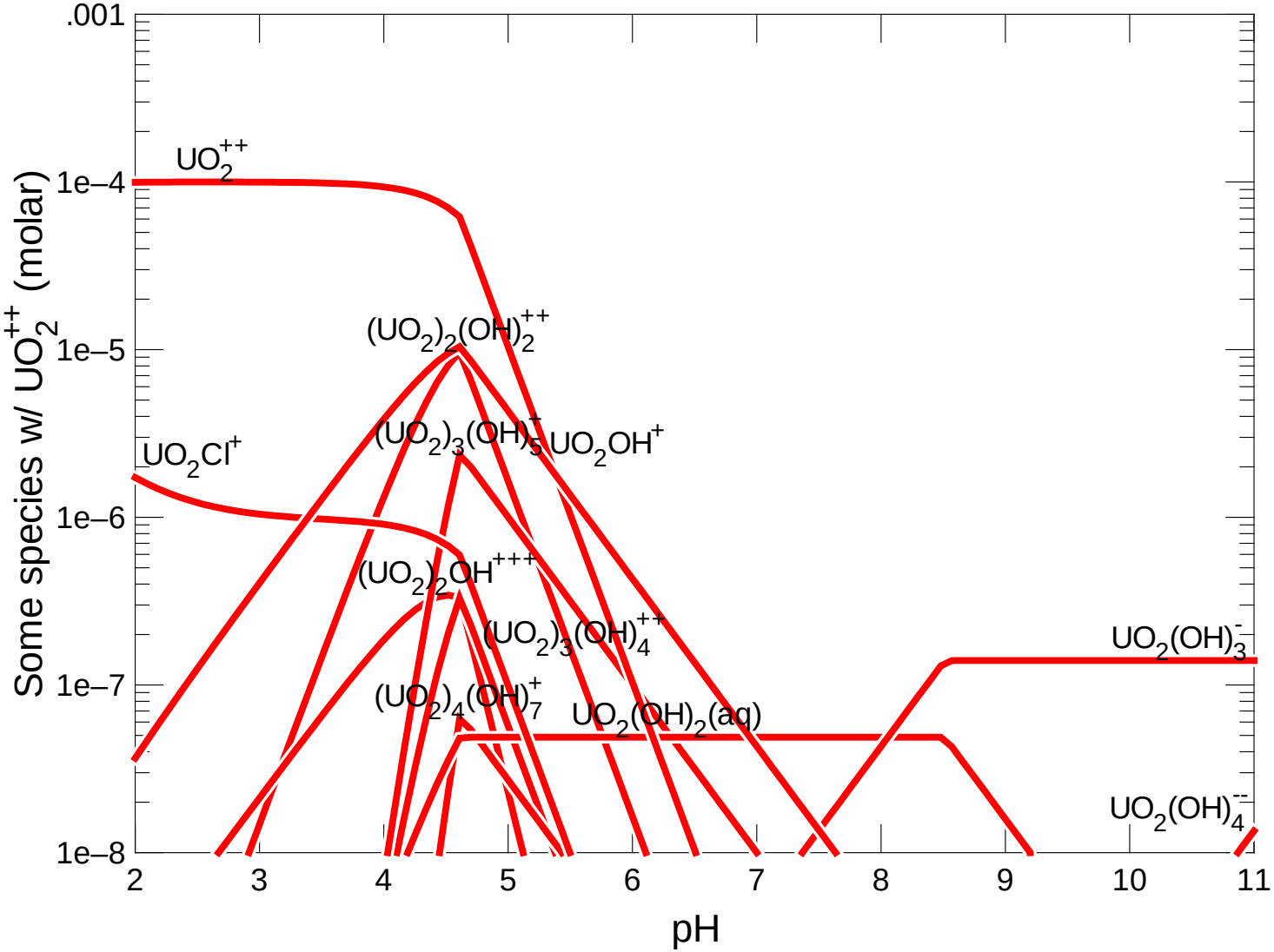

Actinide Halide Complexes (F^-, Cl^-, Br^-, I^-)

- With the exception of F^-, complexes are relatively weak
- Limited data because high ligand concentrations and acidic conditions are required
- Complexation strength
  - $F^- >>> Cl^- > Br^- > I^-$
- Note: In very strong acids, anionic species may form, such as $UO_2(NO_3)_x^{2-x}$, UCl_6^{-2}
- These and similar species are extremely important for separating actinides on ion exchange resins

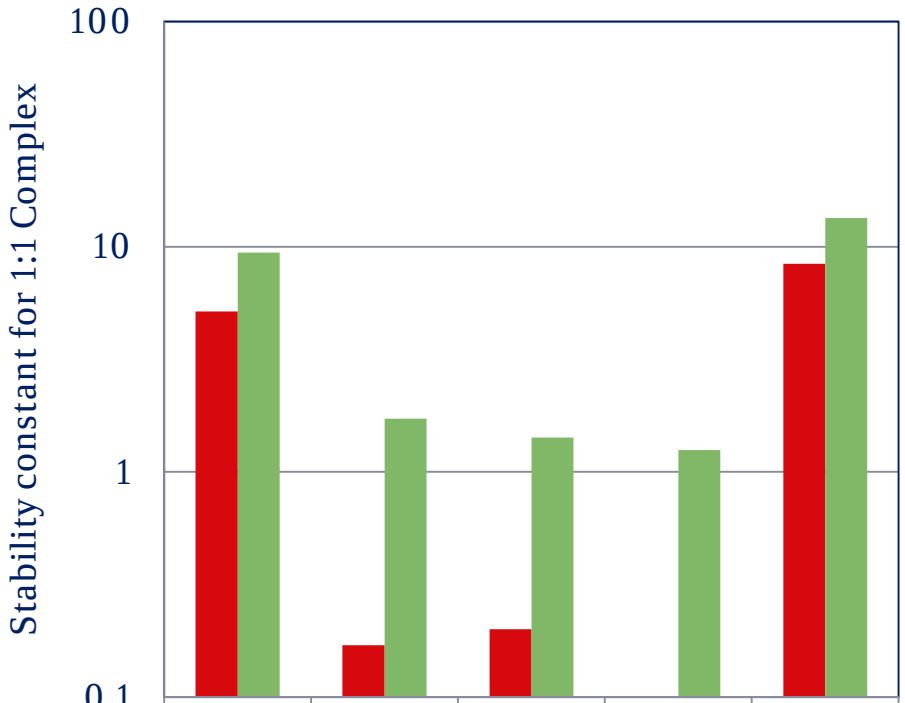

	F-	Cl-	Br-	I-	OH-
U(VI)	5.16	0.17	0.2		8.4
U(IV)	9.42	1.72	1.42	1.25	13.4

Complexation with Oxo-ligands

- General trend:, Cl^-, NO_3^-< F^-, SO_4^{2-}, HPO_4^{2-} < CO_3^{2-}, OH^-
- NO_3^- generally forms stronger complexes than Cl^-
- Primarily due to bidentate binding
- Complexation with other oxo-ligands extremely important for understanding environmental behavior
- Carbonate complexes are of particular importance

$$CO_2(g) \text{ <-> } CO_2(aq) \log K_H = -1.47$$
$$CO_2(aq) + H_2O \text{ <-> } H_2CO_3(aq) \log Keq = -2.70$$
$$H_2CO_3(aq) + H_2O \text{ <-> } H+ + HCO_3^- \log K_1 = -6.35$$
$$HCO_3^- \text{ <-> } H^+ + CO_3^- \log K_2 = -10.33$$

Tetravalent Actinide-Carbonate Complexes

Clark et al., Chem. Rev. 95, 1995, 25-48

Reaction	Ionic Strength	log K
$U^{4+} + 5CO_3^{-} <=> U(CO_3)_5^{6-}$	0	34.0 +/- 0.9
$U(CO_3)_4^{4-} + CO_3^{2-} <=>$	0	-1.12 +/- 0.22
$Th^{4+} + 5CO_3^{2-} <=> Th(CO_3)_5^{6-}$	1	26.2 +/- 0.2
$Pu^{4+} + CO_3^{2-} <=> PuCO_3^{2+}$	0.3	17.0 +/- 0.7
$Pu^{4+} + 2CO_3^{2-} <=> Pu(CO_3)_2^{0}$	0.3	29.9 +/- 0.96
$Pu^{4+} + 3CO_3^{2-} <=> Pu(CO_3)_3^{2-}$	0.3	39.1 +/- 0.82
$Pu^{4+} + 4CO_3^{2-} <=> Pu(CO_3)_4^{4-}$	0.3	42.9 +/- 0.75
$Pu^{4+} + 5CO_3^{2-} <=> Pu(CO_3)_5^{6-}$	0.3	44.5 +/- 0.77
$Pu^{4+} + 2CO_3^{2-} + 4OH^{-} <=> Pu(OH)_4(CO_3)_2^{4-}$	0.1	46.4 +/- 0.70

- $\beta_{1,5}$ U(IV) carbonate complex is approx 8 orders of magnitude greater than $\beta_{1,5}$ Th(IV) carbonate complex
- $\beta_{1,5}$ U(IV) carbonate complex is approx 10 orders of magnitude weaker than $\beta_{1,5}$ Pu(IV) carbonate complex

Comparison of Pu(IV)-CO_3-OH and U(IV)-CO_3-OH Systems

Modeled using Hyss and constants on previous slide

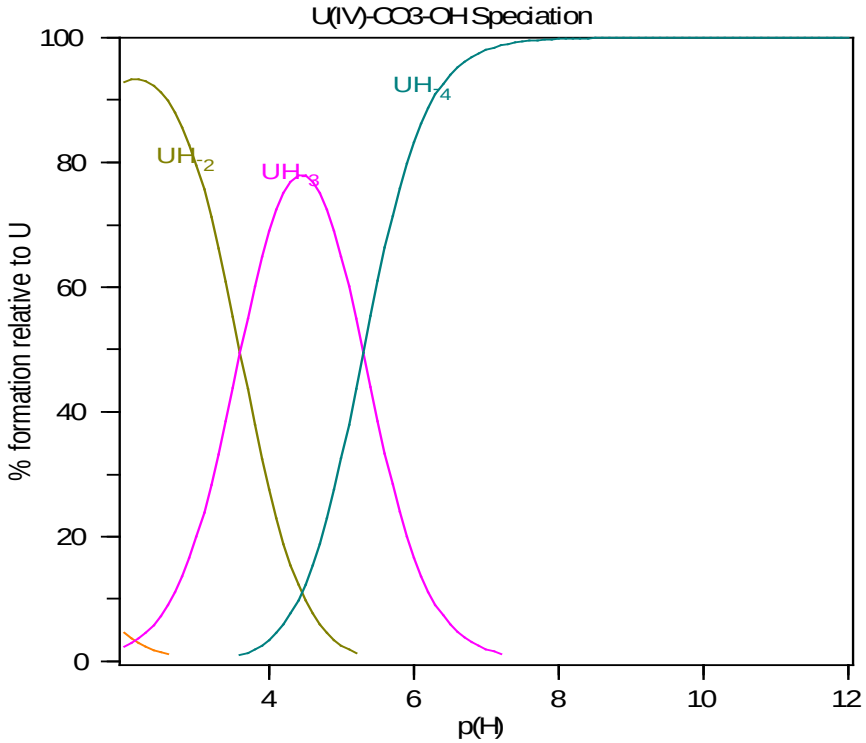

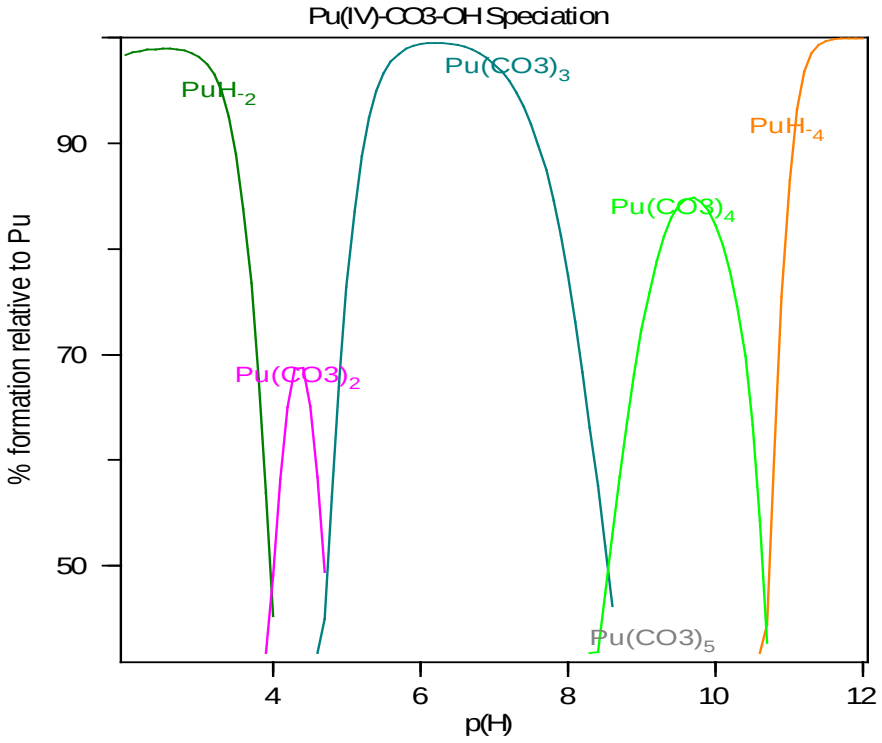

- Due to the higher complexation strength of Pu(IV) relative to U(IV), high carbonate concentrations can prevent hydrolysis at neutral pH values for Pu(IV)
- U(IV) complexation with hydroxide is stronger than carbonate, thus the 1:5 U:CO_3 species does not appear in the plot above.
- System conditions: [Actinide] = 10nM, [CO_3^{2-}] = 10mM

Pentavalent Actinide Carbonate Species

Clark et al., Chem. Rev. 95, 1995, 25-48

Reaction	Ionic Strength	log K
$UO_2^+ + 3CO_3^{2-} <=> UO_2(CO_3)_3^{5-}$	0	7.41 +/- 0.27
$NpO_2^+ + CO_3^{2-} <=> NpO_2CO_3^-$	0.5	4.2 +/- 0.1
$NpO_2^+ + 2CO_3^{2-} <=> NpO_2(CO_3)_2^{3-}$	0.5	6.4 +/- 0.2
$NpO_2^+ + 3CO_3^{2-} <=> NpO_2(CO_3)_3^{5-}$	0.5	7.8 +/- 0.3

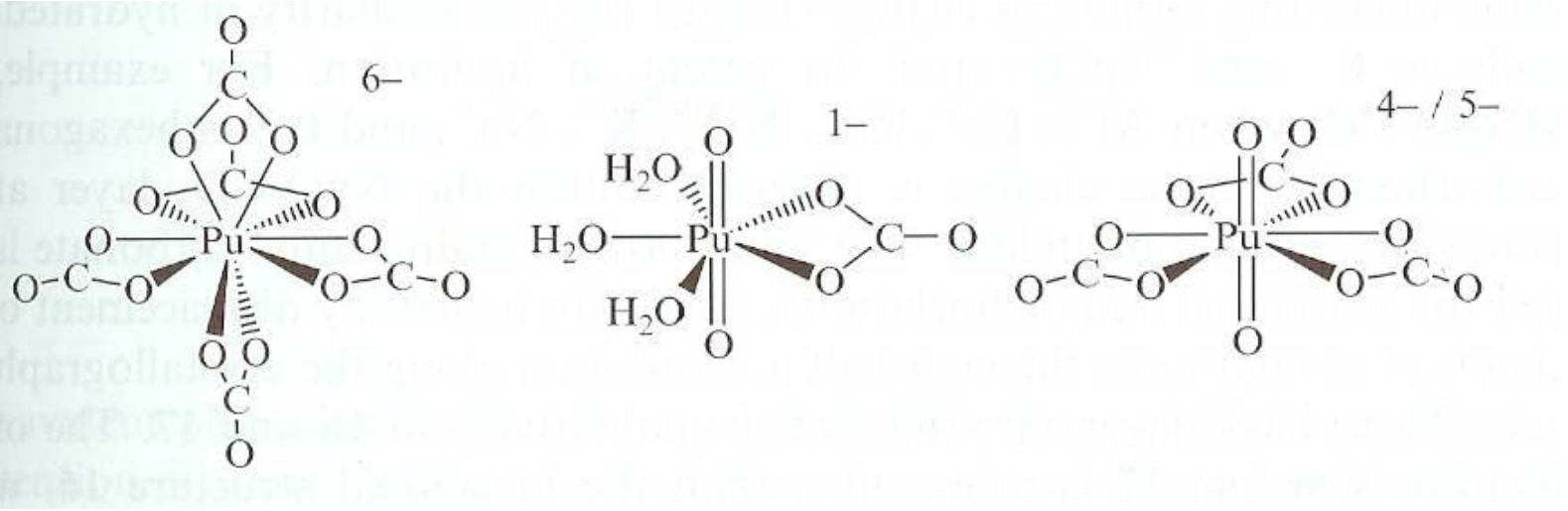

Uranyl Carbonate Species

Clark et al., Chem. Rev. 95, 1995, 25-48

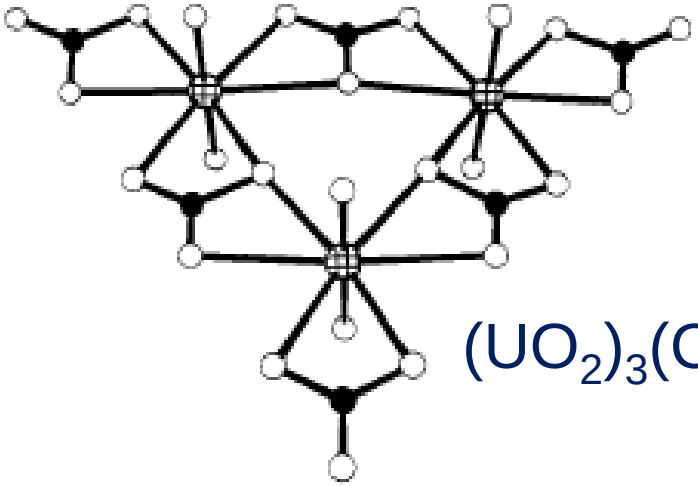

$(UO_2)_3(CO_3)_6^{6-}$

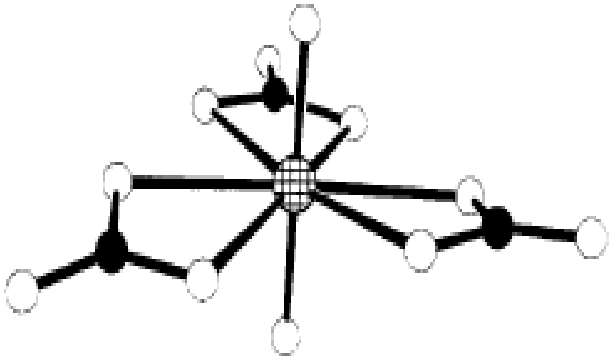

$UO_2(CO_3)_3^{4-}$

Reaction	Ionic Strength	log K
$UO_2^{2+} + CO_3^{2-} <=> UO_2(CO_3)^0$	0	9.68 ± 0.04
$UO_2^{2+} + 2CO_3^{2-} <=> UO_2(CO_3)_2^{2-}$	0	16.94 ± 0.12
$UO_2^{2+} + 3CO_3^{2-} <=> UO_2(CO_3)_3^{4-}$	0	21.60 ± 0.05
$3UO_2^{2+} + 6CO_3^{2-} <=> (UO_2)_3(CO_3)_6^{6-}$	0	54.00 ± 1.00

Uranyl Carbonate Speciation

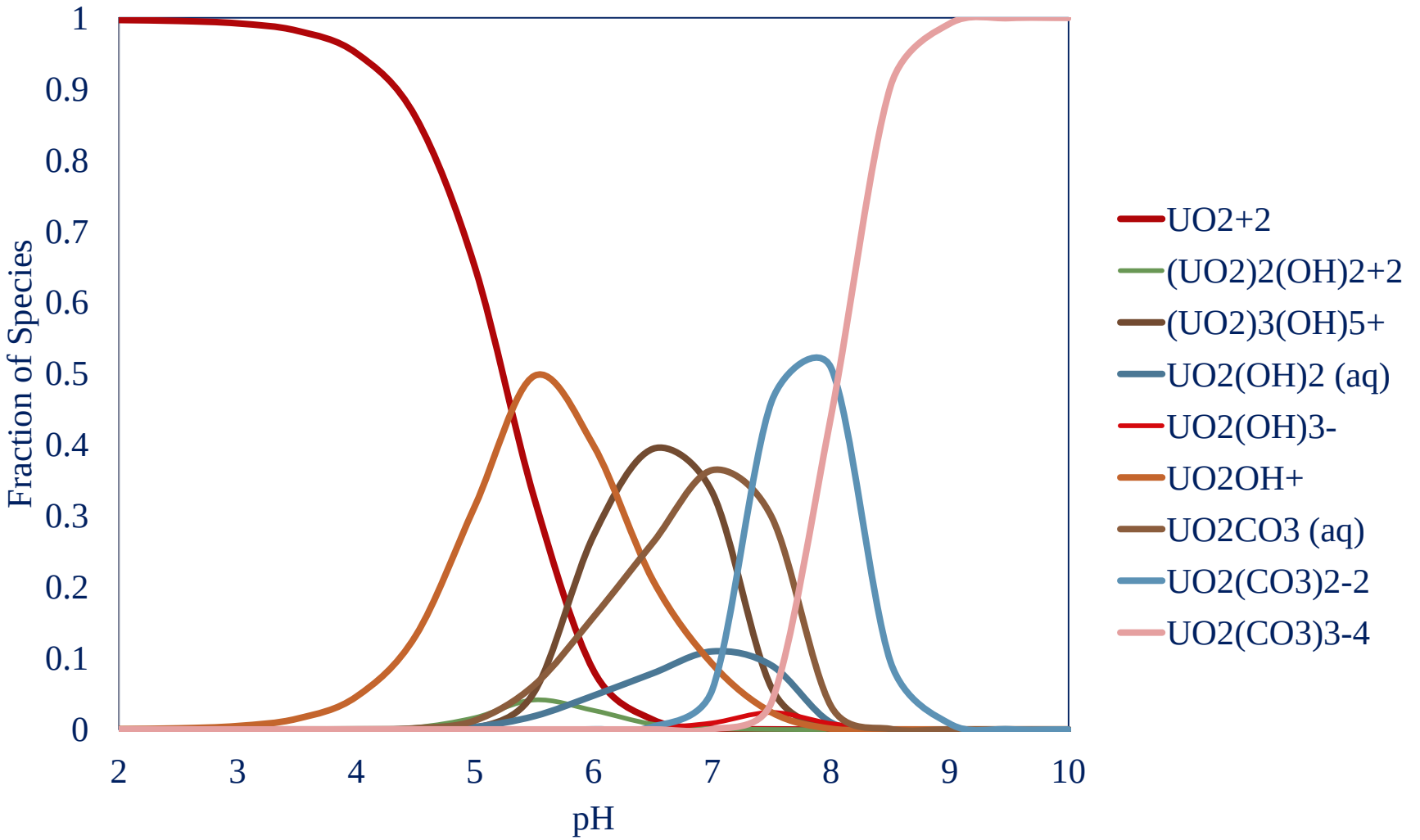

Modeled using Visual MINTEQ, Standard Database
Conditions: 1mM $NaNO_3$, atm CO_2(g), 1μM U(VI)

Ternary Alkali Metal-uranyl-carbonate Species

- Recently, a series of very stable alkali metal-uranyl-carbonate species was identified
- It appears these complexes may be responsible for unexpected results in uranium bioremediation efforts (Brooks et al., 2003)
- The Ca-UO_2-CO_3 species was subsequently identified at environmental concentrations using EXAFS spectroscopy (Kelly et al., 2007)

TABLE 1. Formation Constants of the $MUO_2(CO_3)_3^{2-}$ (aq) and $M_2UO_2(CO_3)_3^0$ (aq) Complexes

	I = 0.1 (mol/L)					I = 0				
	log K_1[a]	log K_2[a]	r^2[b]	Chi^2/DoF[c]	P value[d]	log K_1[e]	log K_2[e]	logβ_{113}[f]	logβ_{213}[f]	reference
Mg^{2+}	2.56 ± 0.01		0.999	1.1×10^{-3}	0.0496	4.27 ± 0.01		26.11 ± 0.04		this work
Ca^{2+}	3.63 ± 0.04	6.29 ± 0.04	0.999	0.24	6.1×10^{-6}	5.34 ± 0.04	8.86 ± 0.04	27.18 ± 0.06	30.70 ± 0.05	this work
		5.0 ± 0.7					7.6 ± 0.7		29.41 ± 0.7	*1*
	2.09 ± 0.25	6.38 ± 0.24				3.8 ± 0.25	8.95 ± 0.24	25.6 ± 0.25	30.79 ± 0.24	*3*
									29.8 ± 0.7	*2*
Sr^{2+}	3.30 ± 0.01		0.998	1.8×10^{-3}	0.46	5.02 ± 0.01		26.86 ± 0.04	-	this work
Ba^{2+}	3.13 ± 0.02	5.34 ± 0.06	0.999	1.8×10^{-3}	2.9×10^{-4}	4.84 ± 0.02	7.91 ± 0.06	26.68 ± 0.04	29.75 ± 0.07	this work

[a] K_1 and K_2 are best fitted values using eq 8 and correspond to the best fitted line showed in Figure 2. [b] Correlation coefficient. [c] Chi^2 is the sum of the squares of the deviations of the theoretical curve from the experimental points, DoF is number of degrees of freedom. [d] P value indicates the probability of incorrectly accepting the quadratic form of eq 8. [e] Corrected values by the Davies equation (*26*). [f] At $I = 0$: $\log \beta_{113} = \log K_1 + \log \beta_{013}$, $\log \beta_{213} = \log K_2 + \log \beta_{013}$, and $\log \beta_{013}$ ($I = 0$) = 21.84 ± 0.04 from ref *15*.

Dong and Brooks, ES&Environ. Sci. Technol., 40 (2006), pp. 4689–4695, 2006;
Brooks et al., Environ. Sci. Technol., 37 (2003), pp. 1850–1858
Kelly et al., Geochimica et Cosmochimica Acta 71 (2007), pp. 821–834

Uranyl Carbonate Speciation

Influence of Ternary Ca-UO2-CO3 Species

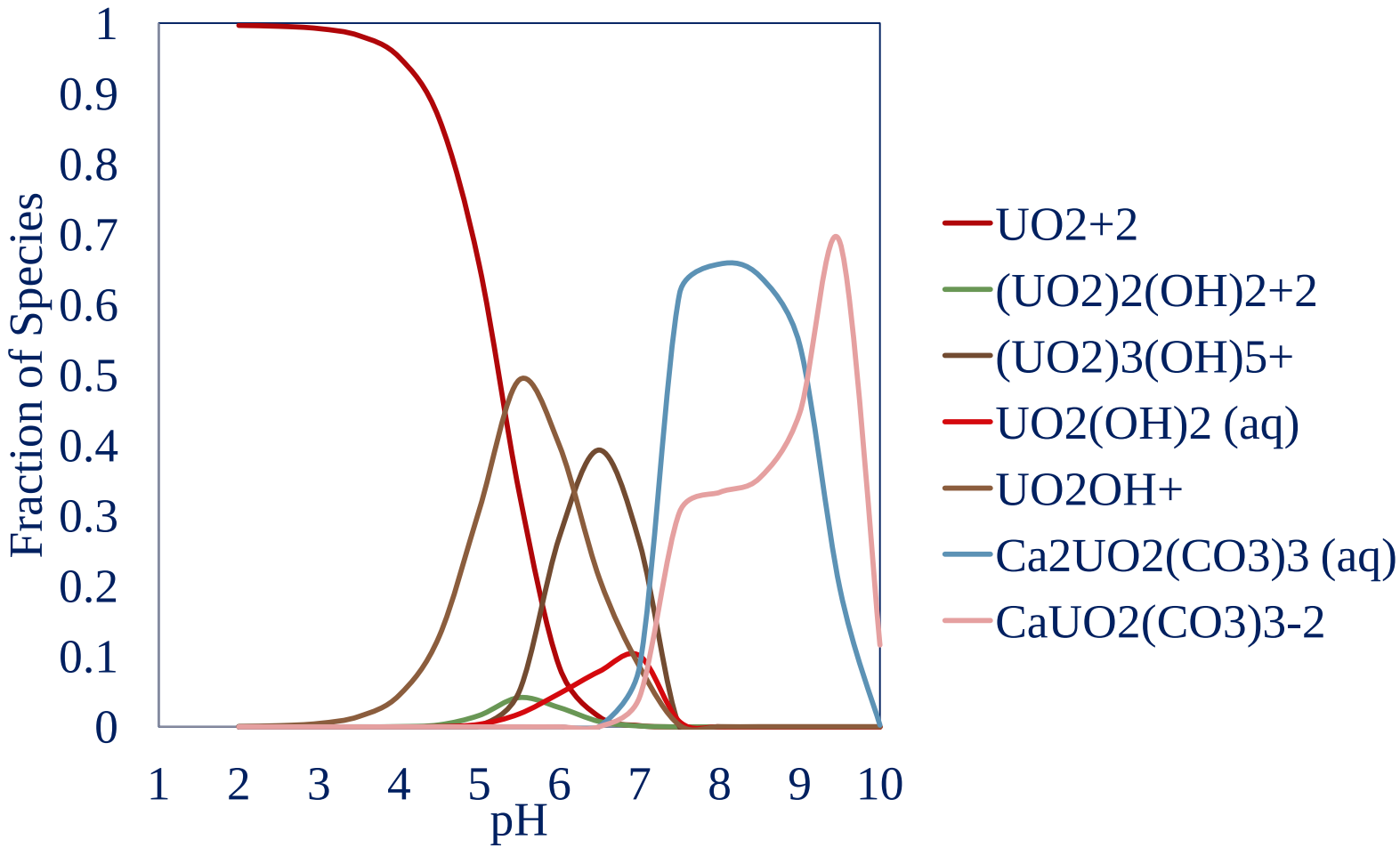

Modeled using Visual MINTEQ, Standard Database
Conditions: 1mM $Ca(NO_3)_2$, atm CO_2(g)

Naturally Occuring Ligands

- Organic materials generated as exudates by organisms and plants and byproducts of decay of organic material
- Aliphatic organics
  - Formic acid (pKa 3.8)
  - Acetic acid (pKa 4.8)
  - Oxalic acid (pKa 1.3)

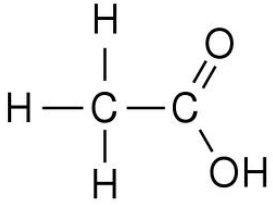

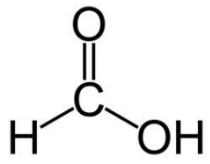

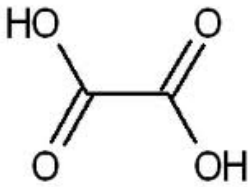

- Amino acids
  - Glycine
  - Aspartic acid
  - Common formula

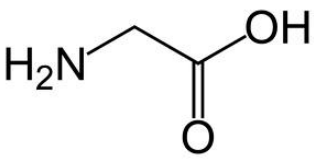

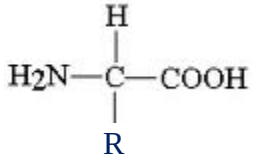

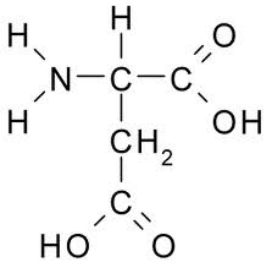

- Saccharides
  - Glucose, cellulose, lignin

Examples of Natural Organic Matter

(DFOB and citric acid shown for comparison)

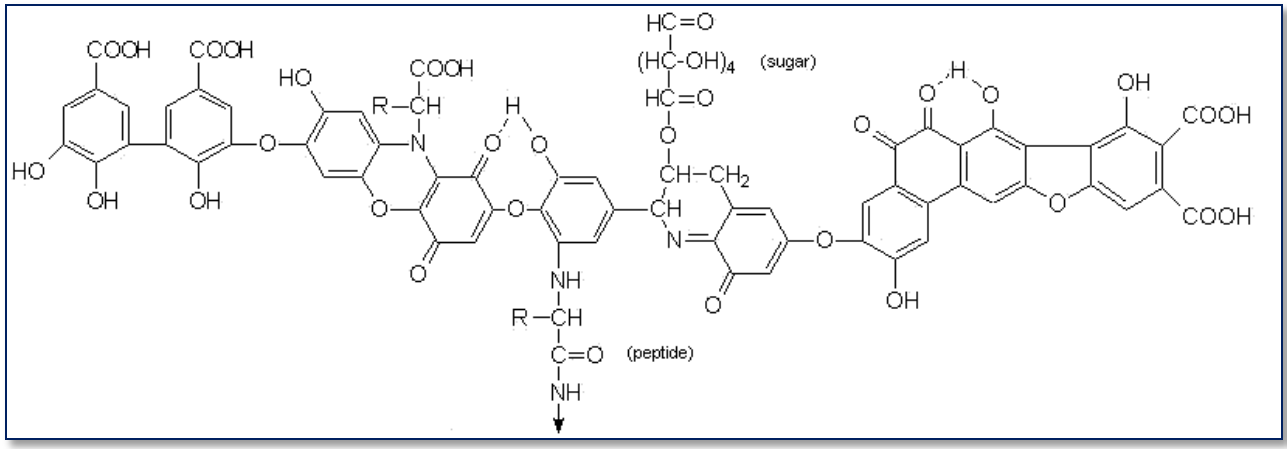

Humic acid (Stevenson 1982)

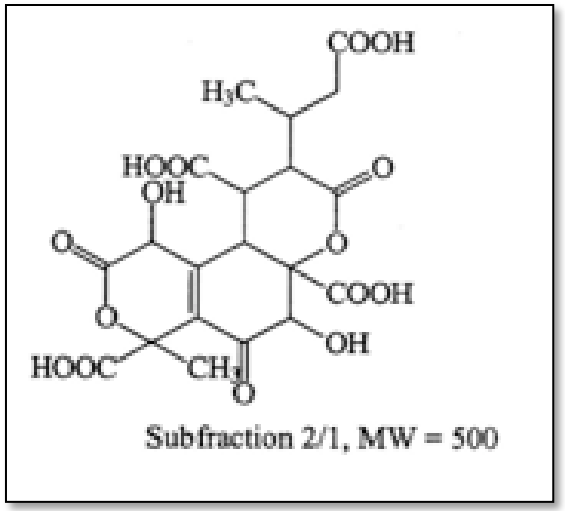

Fulvic acid

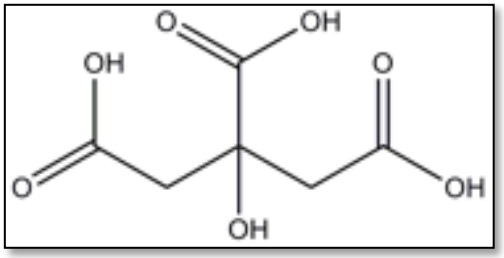

Citric acid

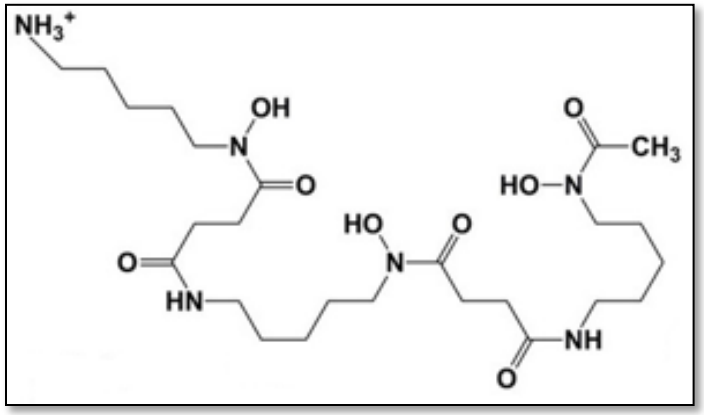

Desferrioxamine-B

U(VI) - Citric Acid Complexation

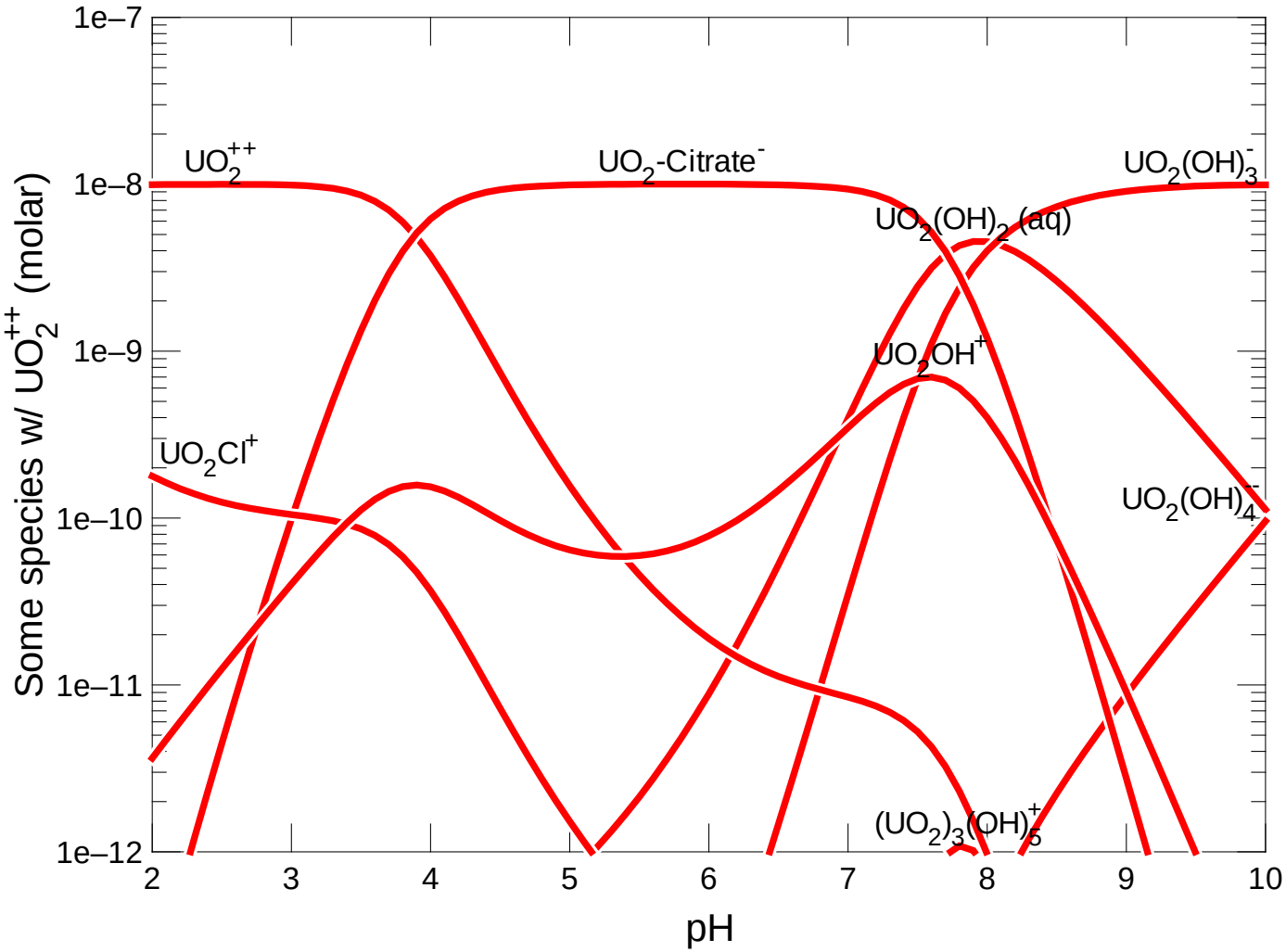

- Modeled using Geochemist workbench
- Conditions: [U(VI)] = 1uM, [NaCl] = 10 mM, [citric acid] = 10 uM

Humic Acid – Actinide Complexation

Silva and Nitsche, 1995, Radiochim. Acta

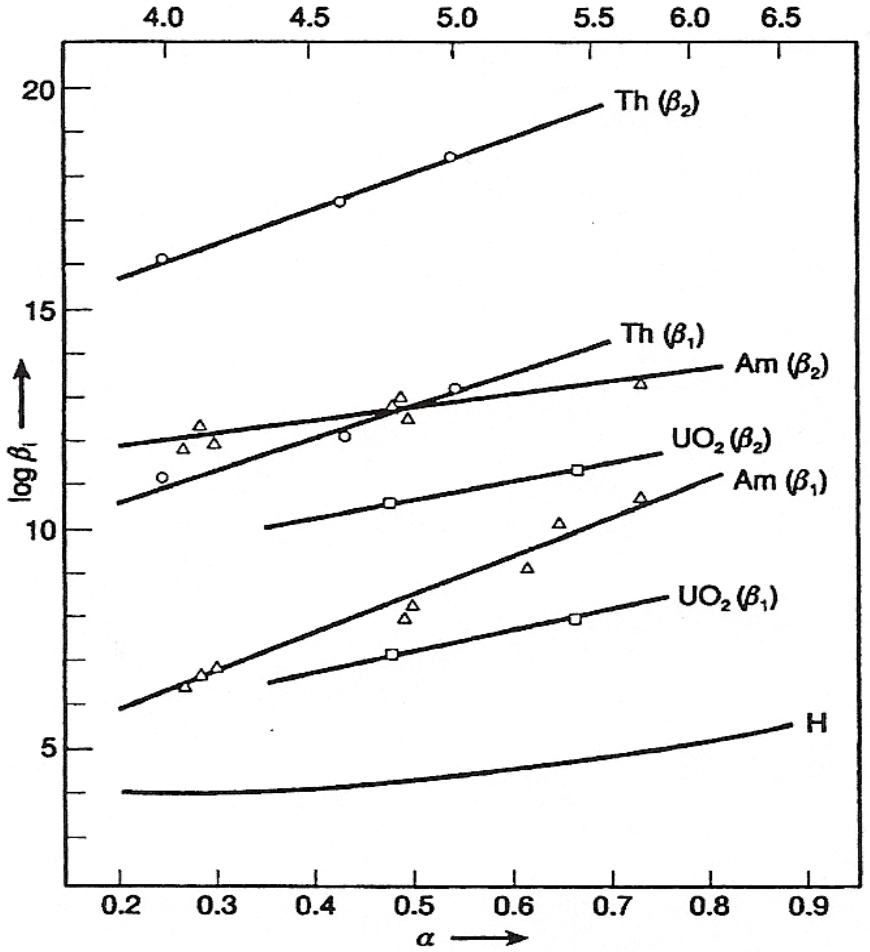

Figure 6.11 Complex formation constants of several actinides with humic acid as a function of the degree of ionization (α) and pH. (Reprinted from Ref. 75 with permission from the author.)

Oxidation/Reduction – Outline

- Common oxidation states
- Redox speciation in natural waters

Uranium Oxidation/Reduction

- Oxidation state has profound influence on U mobility
  - $U(IV)^{4+} << U(VI)O_2^{2+} \approx U(III)^{3+} < U(V)O_2^{+}$

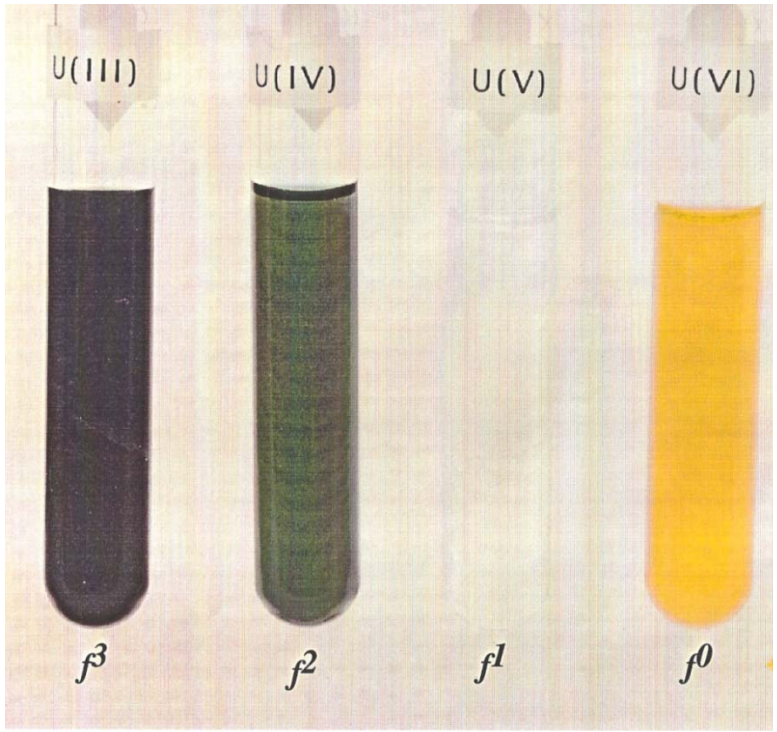

$U(OH)_x^{(4-x)}$ $\quad O=U^{+}=O$

$U(OH)_x^{(3-x)}$ $\quad O=U^{++}=O$

Uranium E_H-pH Diagram, Closed System

GWB Model, LLNL Database

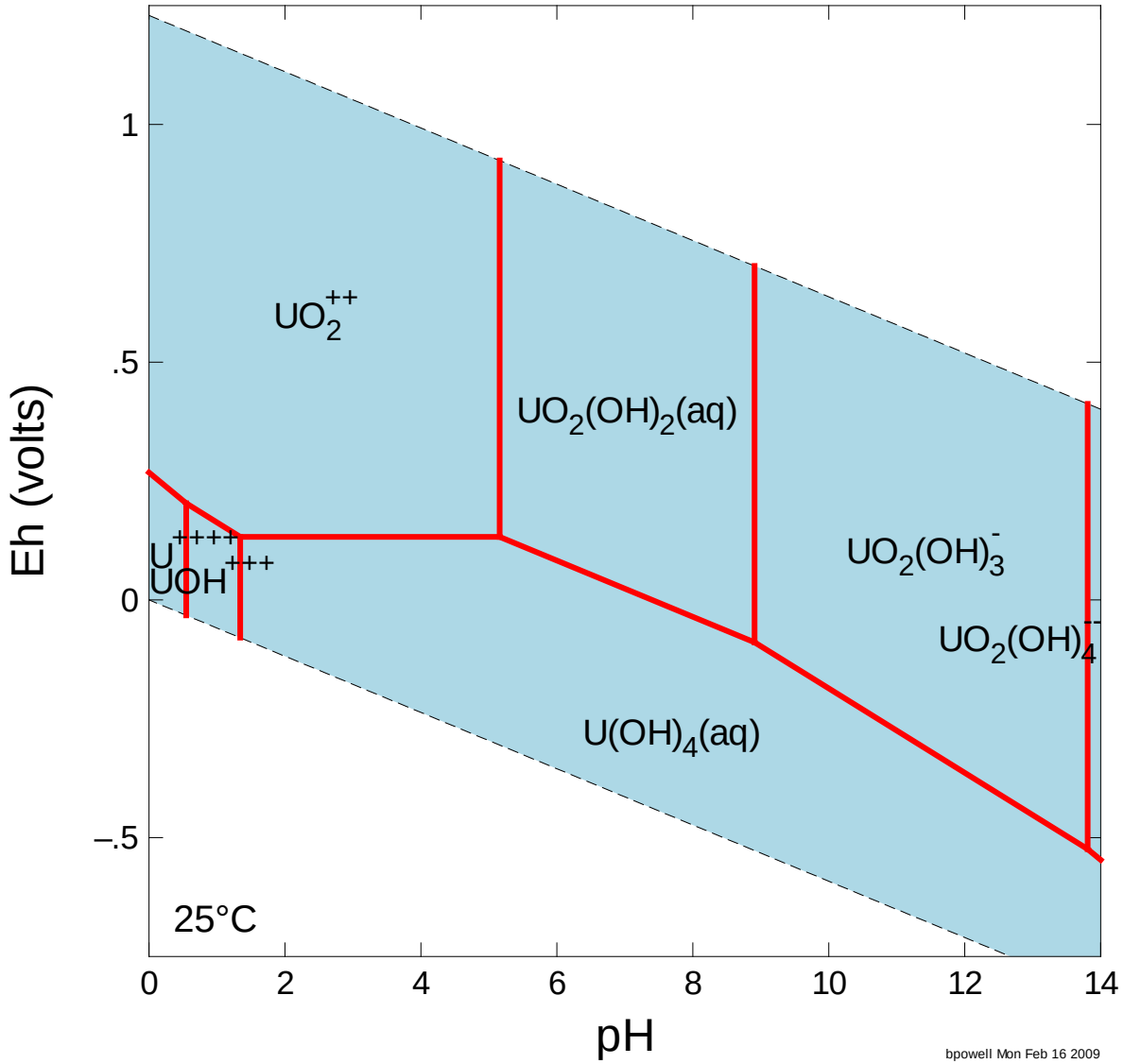

Note: The species shown is the species representing the majority of the analyte in the system. There could be other species present at significant concentrations which are not shown. Think about these diagrams as you are looking "down" on a speciation versus pH diagram.

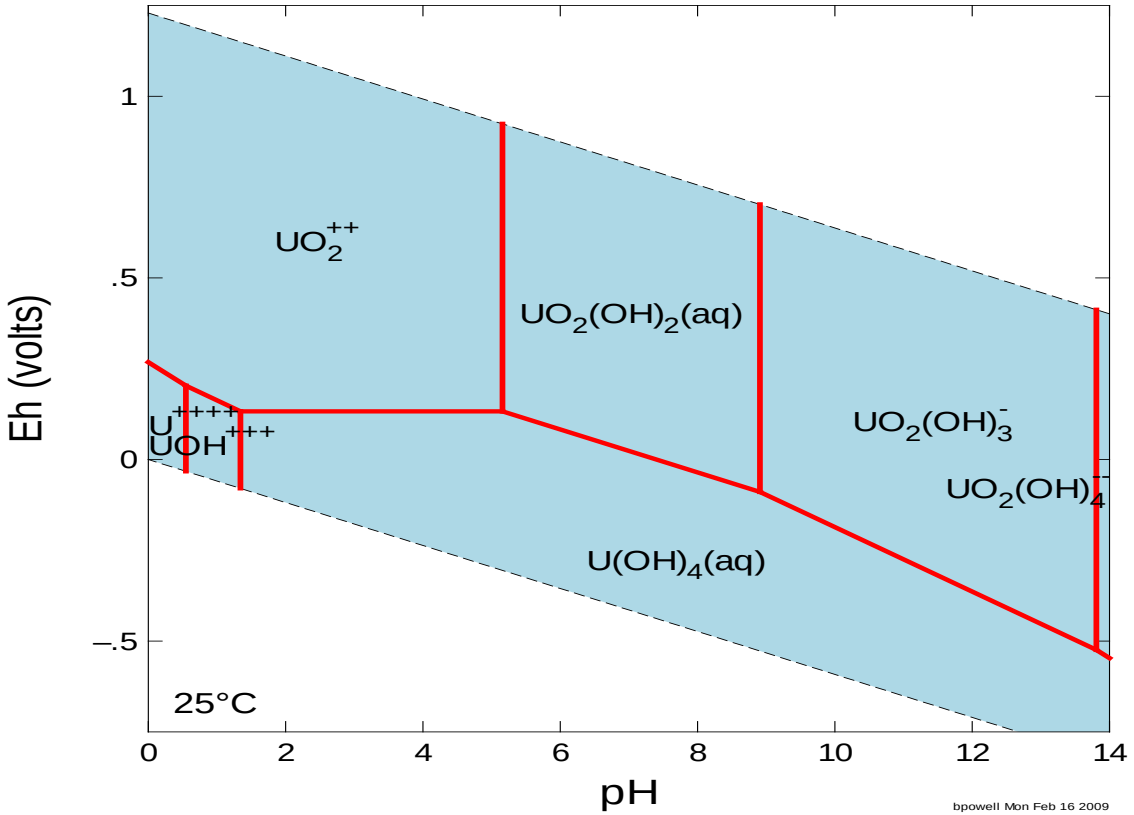

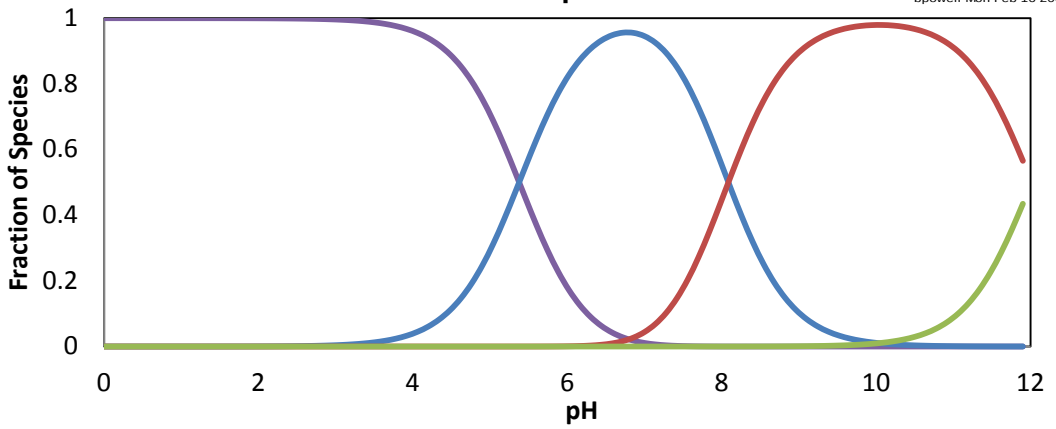

Uranium Speciation versus pH

Modeled with GWB, LLNL Database, [U(VI)]total= 1E-10 M

Note: The species shown is the species representing the majority of the analyte in the system. There could be other species present at significant concentrations which are not show. Think about these diagrams as you are looking "down" on a speciation versus pH diagram.

Uranium E_H-pH Diagram, Open System

GWB Model, LLNL Database

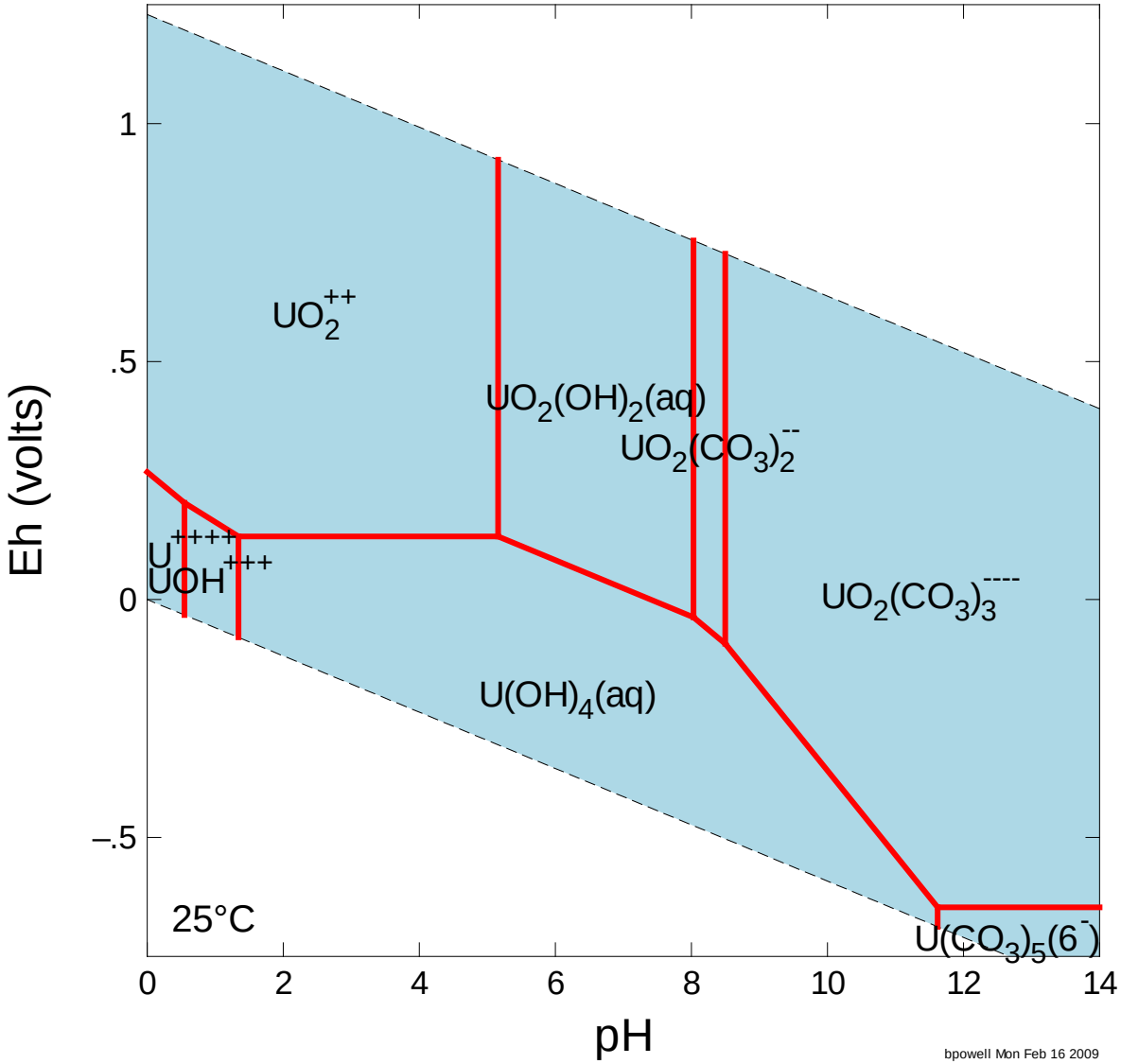

Uranium Reduction by AH_2DS

Wang et al., RCA, 2008, 599-605

- Maximum U(VI) reduction rate followed the order: $OH^- > CO_3^{--} > EDTA > DFOB$
- Reverse trend of the thermodynamic stability of the complex

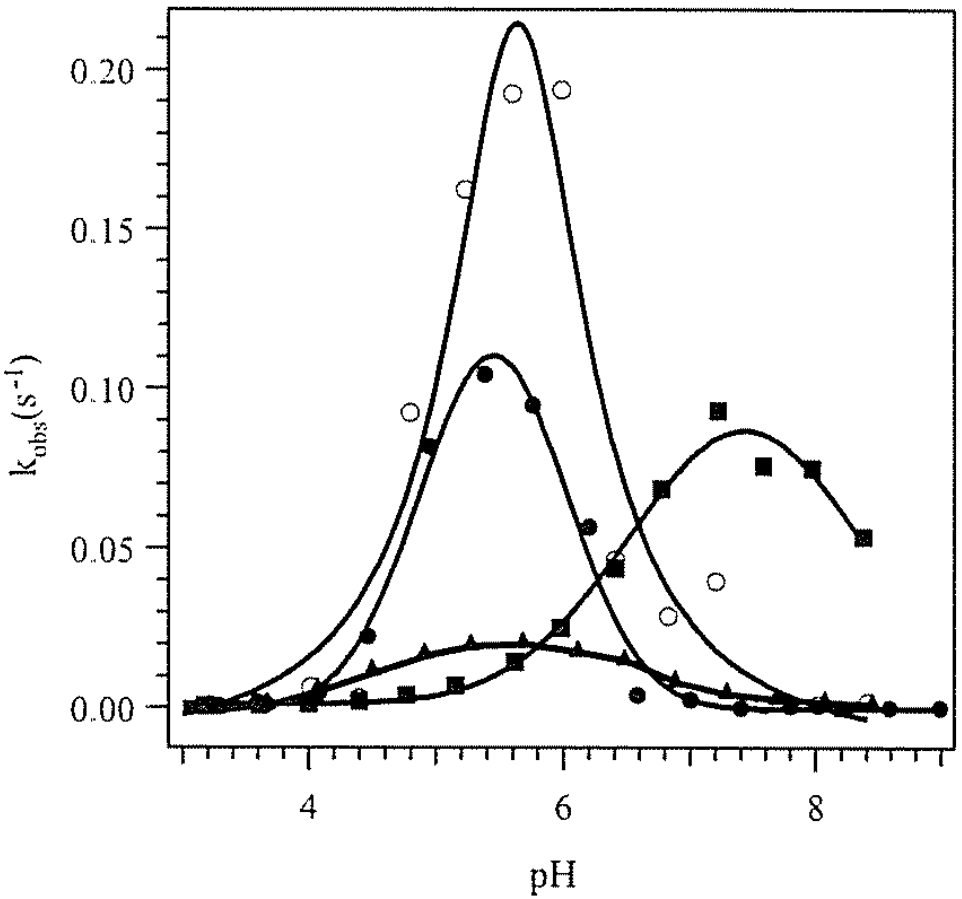

Fig. 4. Observed *pseudo*-1st-order rate constants of U(VI) reduction by AH_2DS as a function of pH in four systems (open circle – OH^-, filled circle – carbonate, filled triangle – DFB, filled square – EDTA). The solid lines are fitted trend lines with arbitrary functions.

Np Reduction by Quinonoid Enriched Humic Derivatives

Shcherbina et al., Env. Sci. Tech., 41, 7010-7015, 2007

TABLE 1. Functional Groups Content and Redox Capacity of the Humic Derivatives Used (*27*)

sample	description	−COOH[a], mmol/g	−ArOH[b], mmol/g	redox capacity[c], mmol/g
CHP	Leonardite HA	4.2 ± 0.2	1.1	0.6 ± 0.1
	copolymers of CHP with hydroquinone			
HQ100	HQ:CHP ratio of 100:1000 mg	4.3 ± 0.3	4.0	1.2 ± 0.2
HQ250	HQ:CHP ratio of 250:1000 mg	3.6 ± 0.1	4.4	2.9 ± 0.1
HQ500	HQ:CHP ratio of 500:1000 mg	3.1 ± 0.2	4.3	4.0 ± 0.1
	copolymers of CHP with catechol			
CT500	CT:CHP ratio of 500:1000 mg	3.6 ± 0.8	4.6	2.9 ± 0.4
	copolymers of CHP with p-benzoquinone			
BQ500	BQ:CHP ratio of 500:1000 mg	3.9 ± 0.1	4.1	2.0 ± 0.1

[a] Determined by calcium acetate method (30). [b] Calculated as a difference between total acidity and −COOH content (30). [c] Cetermined as described in ref 31 using ferricyanide as an oxidant.

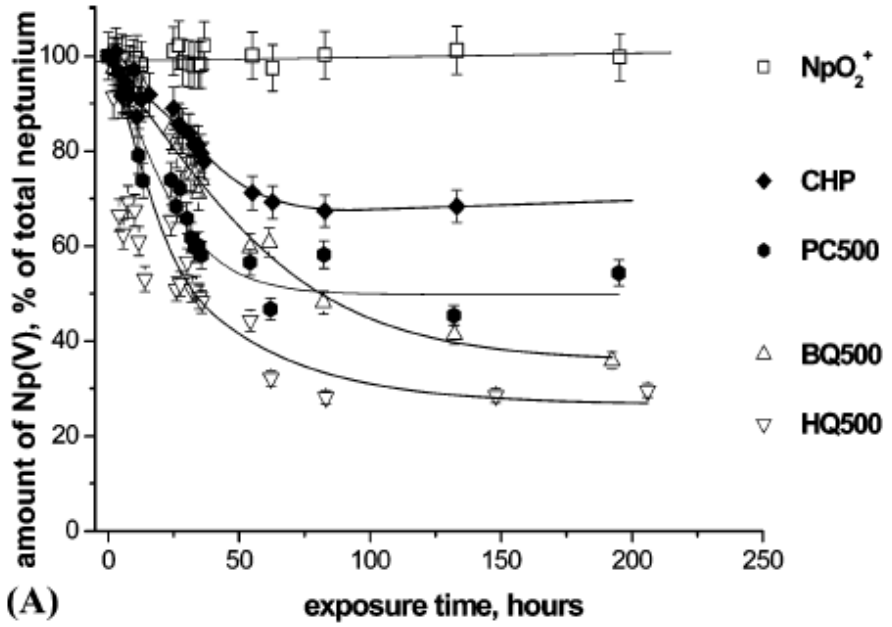

FIGURE 2. Reduction of Np(V) by humic derivatives under anoxic conditions and pH 4.7, $C_0(Np) = 5.4 \times 10^{-5}$ M, $C_0(HS) = 500$ mg/L, Np(V):HS ratio = 1:40. A, Effect of quinonoid monomer nature incorporated into humic structure; B, Effect of different parent HA-to-monomer ratio for HQ enriched derivatives.

Sorption/Desorption

- Overview of mineral water interface chemistry
- Quantifying sorption processes
- Sorption in binary systems
- Influence of aqueous chemistry on sorption
  - Aqueous complexation with inorganic ions
  - Redox reactions complexation on sorption
  - Complexation with organic ions
- Colloidal transport of plutonium

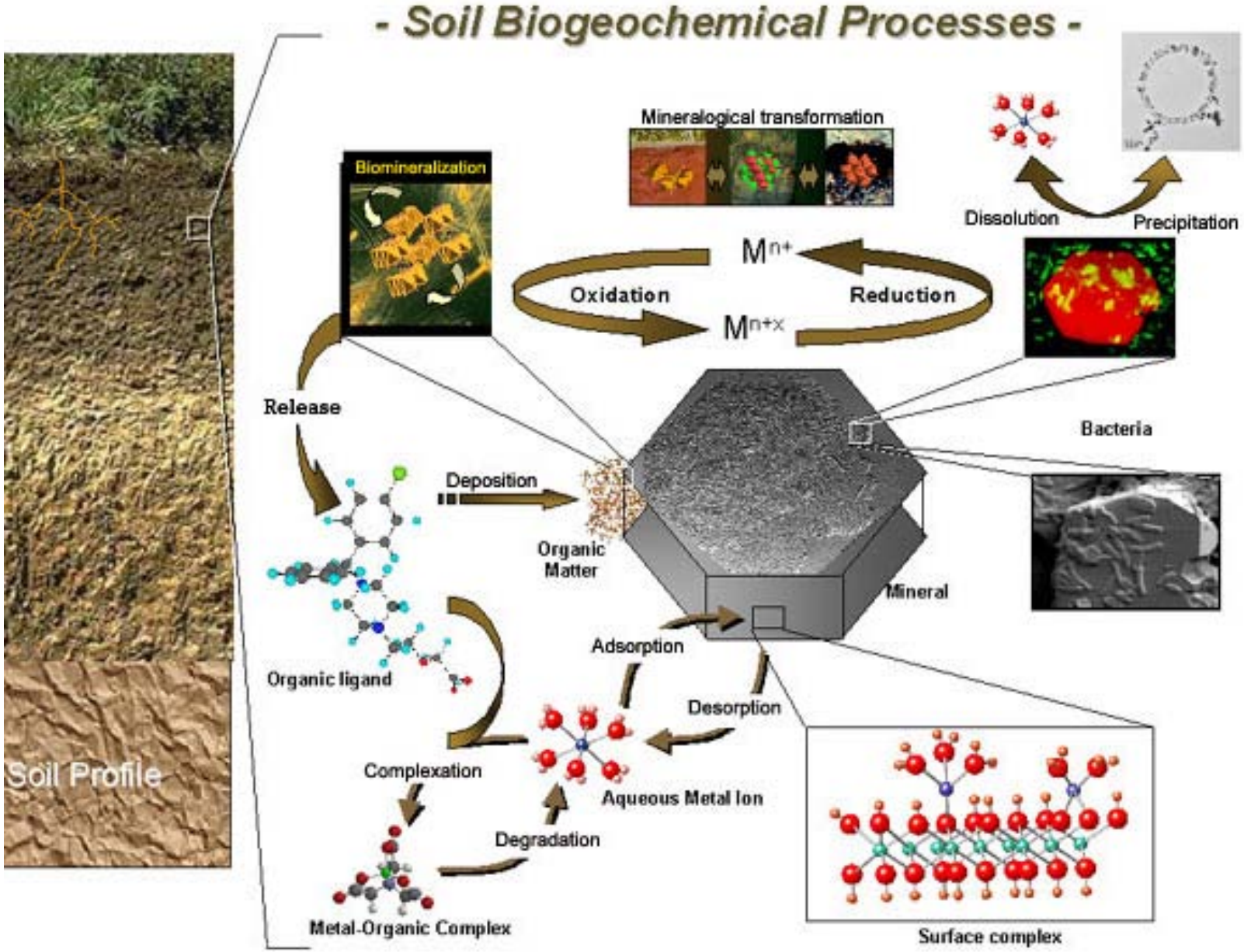

Scott Fendorf Soil and Biogeochemisry Research http://soils.stanford.edu/

Sorption Distribution Coefficients

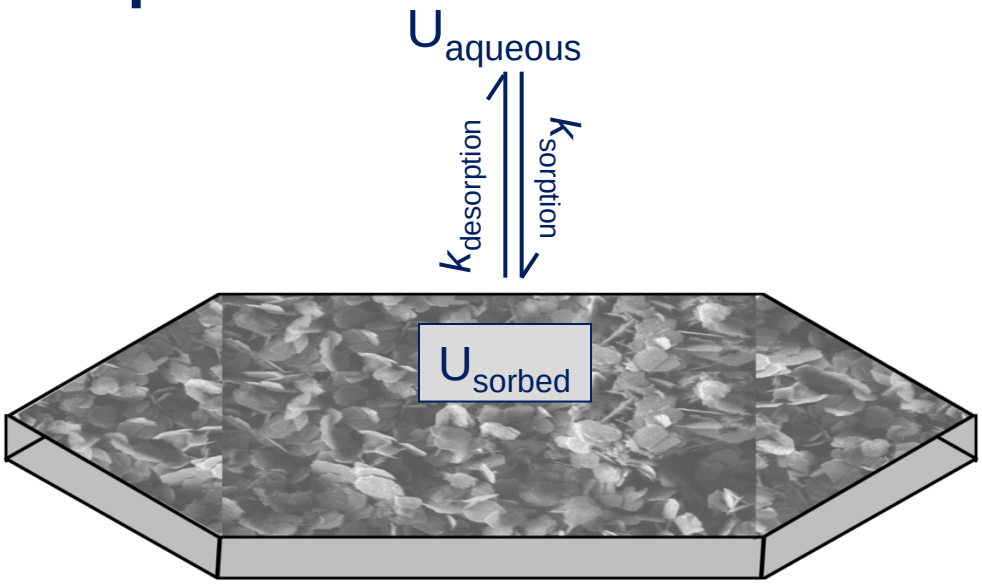

$$K_D = \frac{\text{U Sorbed Conc.}}{\text{U Aqueous Conc.}}$$

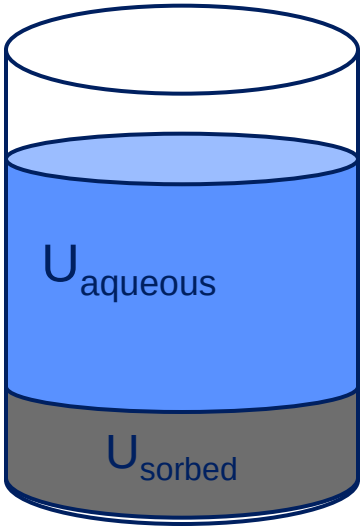

Filter sample at time (t) and measure aqueous U concentration

$$K_D = \left[\frac{[U]_o - [U]_t}{[U]_t} \right] \frac{V}{m}$$

$[U]_o$ = initial aqueous U conc.
$[U]_t$ = aqueous U conc. at time t
V = solution volume
m = mass of solid phase

Empirically Quantifying Sorption Processes

- Linear Distribution Coefficient, K_d

$$K_d = \frac{[An(t)]_{solid}}{[An(t)]_{aqu}}$$

  - Typically determine $[An(t)]_{solid}$ by difference during sorption tests

$$[An(t)]_{solid} = ([An]_{total} - [An(t)]_{aqu}) * \frac{Volume_{aqu}}{mass_{solids}}$$

- Empirical Isotherms

  - Freundlich $\quad [An(t)]_{solid} = K_f [An(t)]^n_{aqu}$

  - Langmuir $\quad [An(t)]_{solid} = \frac{[An(\max)]_{solid} K_l [An(t)]_{aqu}}{1 + K_l [An(t)]_{aqu}}$

Langmuir Sorption Isotherm

Stumm and Morgan, 1996, Chapter 9

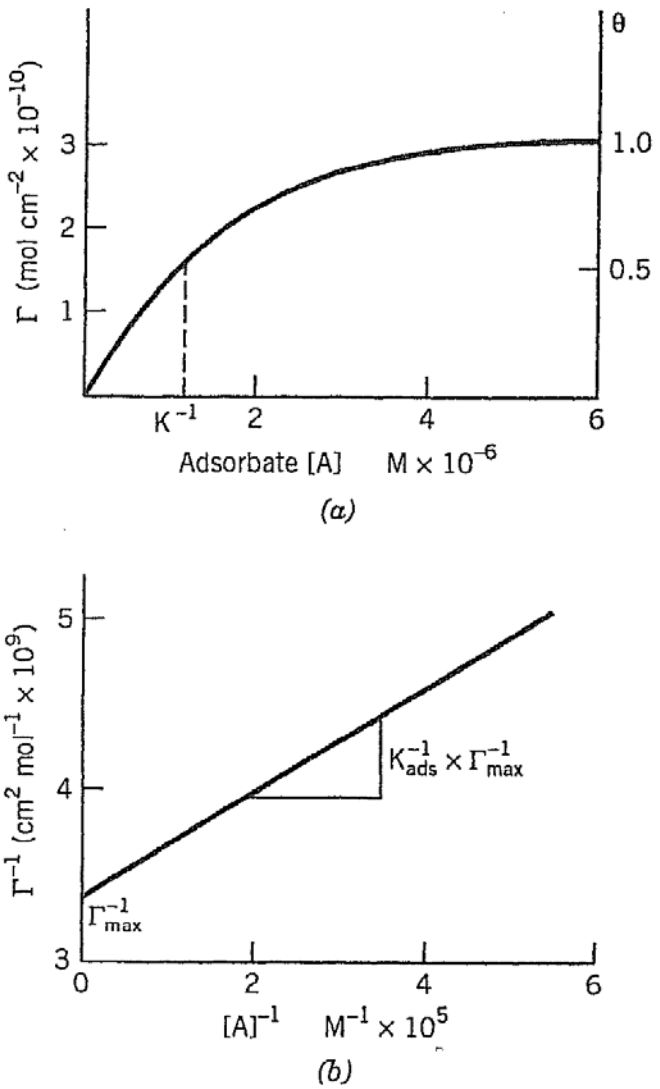

Figure 9.1. Langmuir adsorption isotherm. From the adsorption isotherm (plotted in accordance with equation 11a or equation 11b), the equilibrium constant K_{ads} and the adsorption capacity, Γ_{max}, are obtained by plotting Γ^{-1} versus the reciprocal concentration (activity) of the adsorbate (equation 11c).

Freundlich and Langmuir Sorption Isotherms

(Stumm and Morgan, 1996, Chapter 9)

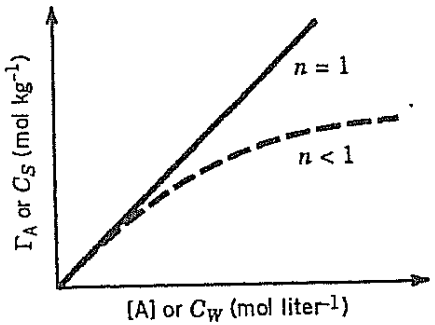

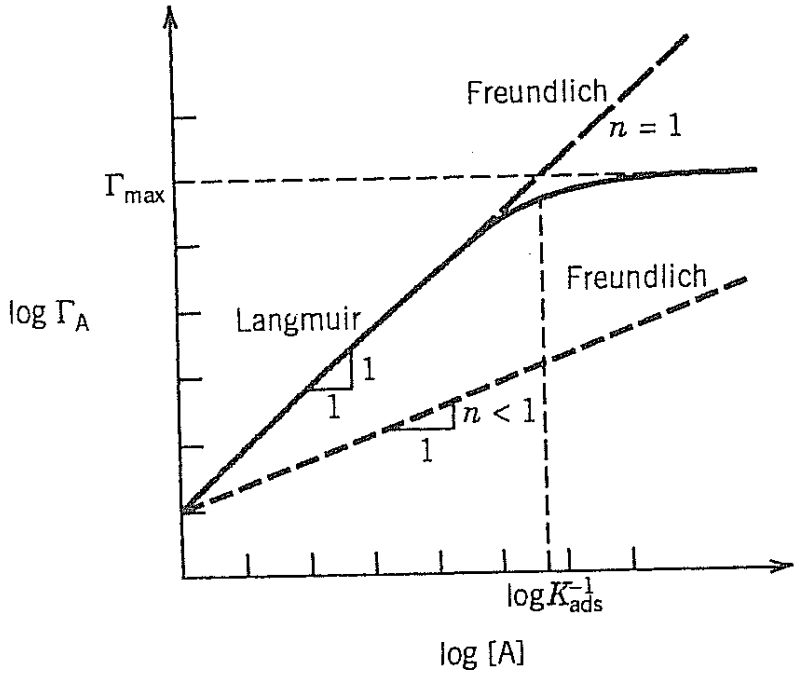

Figure 9.2. Plot of adsorption data in a double logarithmic plot. In a Langmuir isotherm the initial slope is unity. A Freundlich isotherm shows in a double log plot a slope of $n < 1$. Such a Freundlich isotherm is obtained if the adsorbent is heterogeneous (decreasing tendency for adsorption with increasing q). (Adapted from Morel, 1983.) *Inset:* Observed relationship between the concentrations of a chemical in the sorbed state Γ or C_s and the dissolved state [A] or C_w.

Surface Complexation Reactions

$\Delta G = -RT \ln K$

$\Delta G_{rxn} = \Delta G_{chemical} + \Delta G_{electrostatic}$

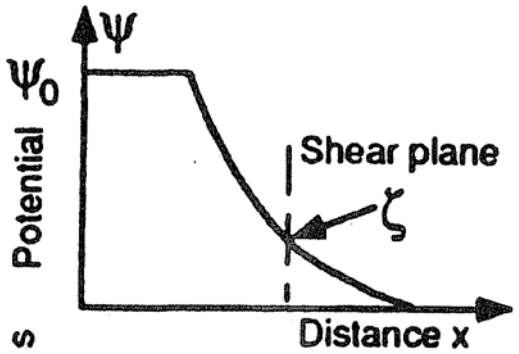

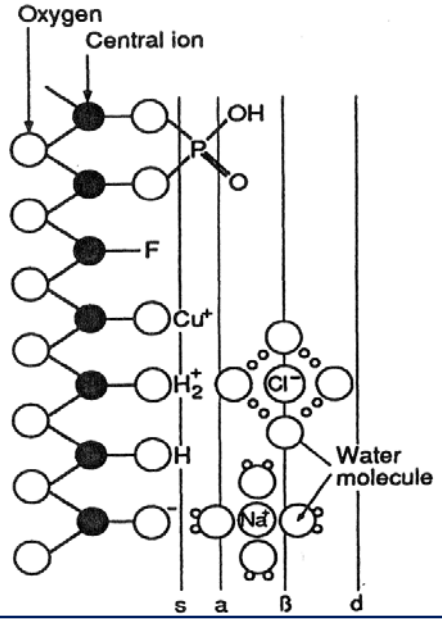

$\equiv SOH + H^+ \Leftrightarrow \equiv SOH_2^+$	$K_+ = \frac{[SOH_2^+]}{[SOH]\{H^+\}} \exp\left(\frac{F\psi}{RT}\right)$
$\equiv SOH \Leftrightarrow \equiv SO^- + H^+$	$K_- = \frac{[SO^-]\{H^+\}}{[SOH]} \exp\left(-\frac{F\psi}{RT}\right)$
$\equiv SOH + M^{n+} \Leftrightarrow \equiv SOM^{n-1} + H^+$	$K_{M^+} = \frac{[SOM^{n-1}]\{H^+\}}{[SOH]\{M^{n+}\}} \exp\left((n-1)\frac{F\psi}{RT}\right)$

Figures from Stumm, *Chemistry of the Solid Water Interface*

Surface Complexation Reactions

Table 9.1. Adsorption (Surface Complex Formation Equilibria)

Acid–Base Equilibria		
$S{-}OH + H^+$	$\rightleftharpoons$	$S{-}OH_2^+$
$S{-}OH\ (+ OH^-)$	$\rightleftharpoons$	$S{-}O^- + (H_2O)$
Metal Binding		
$S{-}OH + M^{z+}$	$\rightleftharpoons$	$S{-}OM^{(z-1)+} + H^+$
$2\ S{-}OH + M^{z+}$	$\rightleftharpoons$	$(S{-}O)_2M^{(z-2)+} + 2\ H^+$
$S{-}OH + M^{z+} + H_2O$	$\rightleftharpoons$	$S{-}OMOH^{(z-2)+} + 2\ H^+$
Ligand Exchange (L^- = ligand)		
$S{-}OH + L^-$	$\rightleftharpoons$	$S{-}L + OH^-$
$2\ S{-}OH + L^-$	$\rightleftharpoons$	$S_2{-}L^+ + 2\ OH^-$
Ternary Surface Complex Formation		
$S{-}OH + L^- + M^{z+}$	$\rightleftharpoons$	$S{-}L{-}M^{z+} + OH^-$
$S{-}OH + L^- + M^{z+}$	$\rightleftharpoons$	$S{-}OM{-}L^{(z-2)+} + H^+$

Source: Adapted from Schindler and Stumm (1987).

Stumm and Morgan, 1996

Surface Charge Versus pH

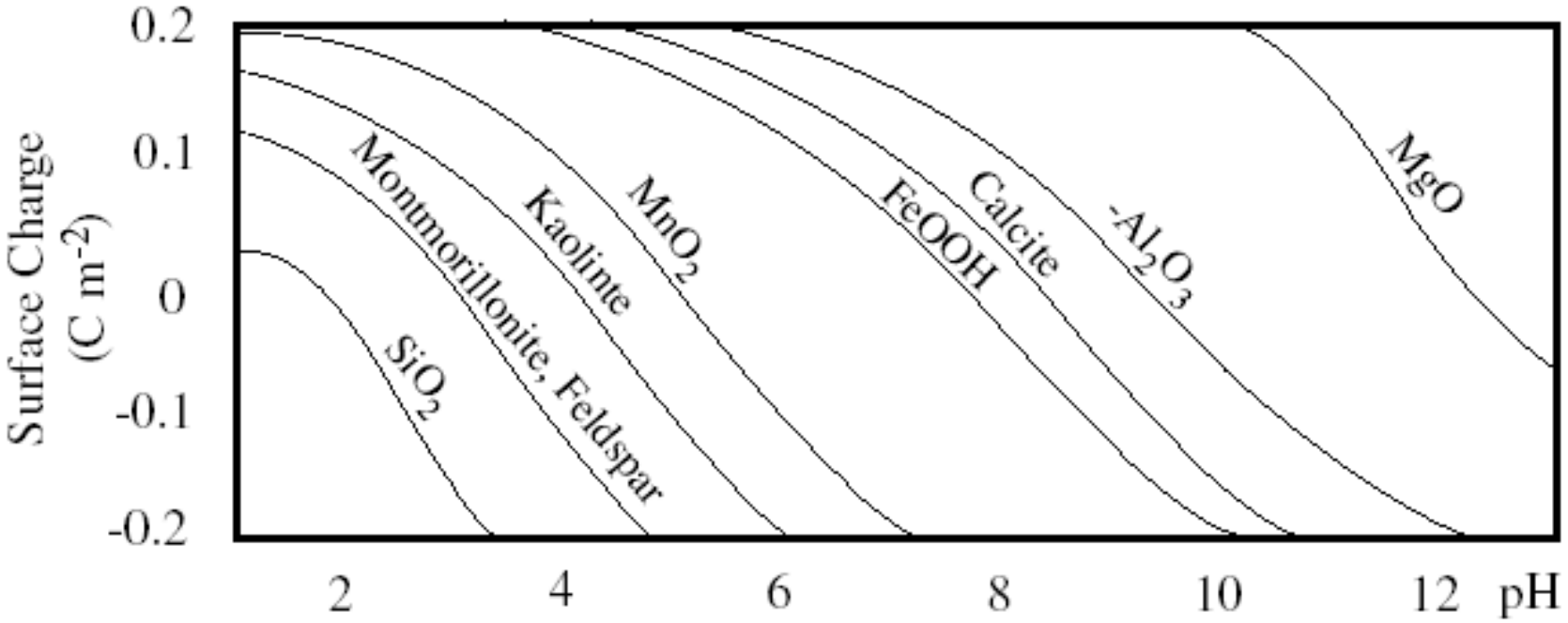

Modified from Stumm and Morgan, 1996

Cation Sorption: Actinide Sorption Trends

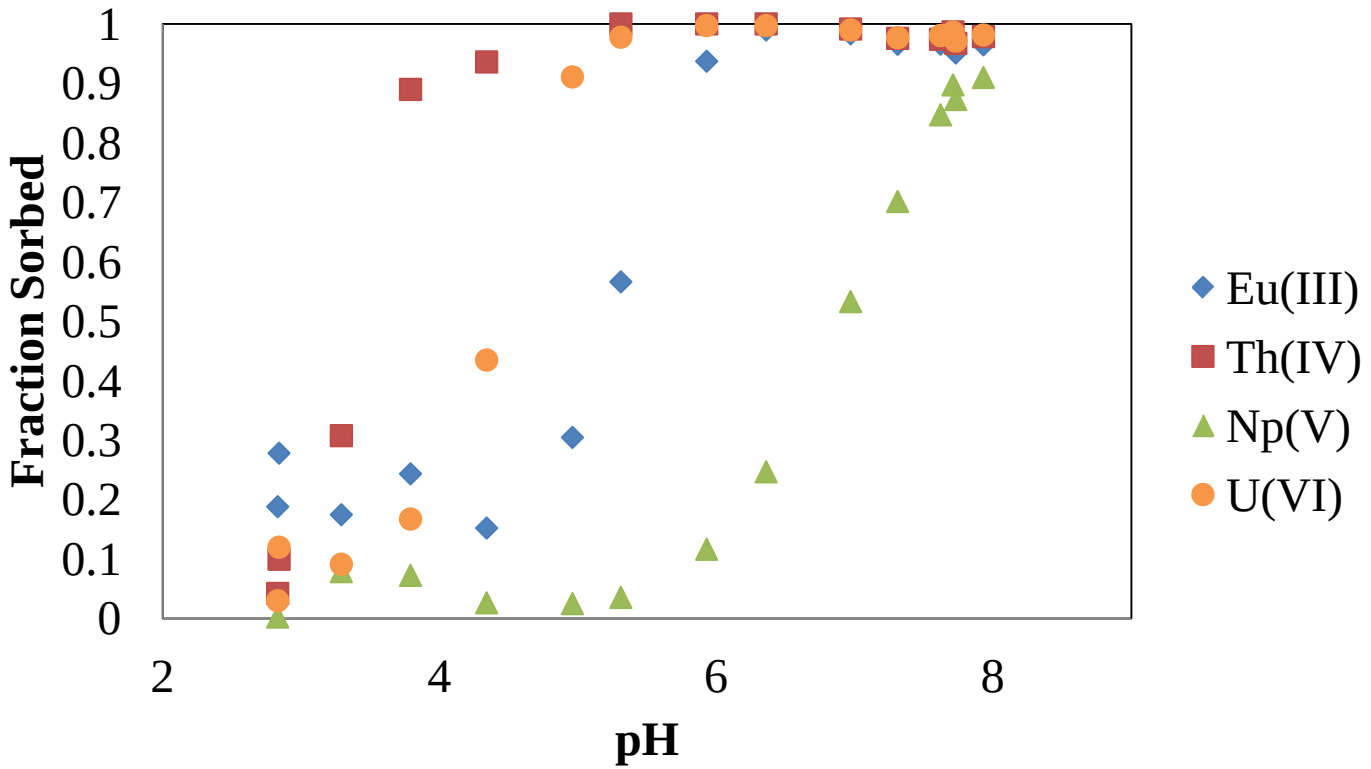

- Sorption of actinides to goethite versus pH
  - Unpublished data from Shanna Estes, Clemson University, 2011
- Sorption affinity follows expected trend
- An(IV) > An(VI) > An(III) > An(V)

Effect of Carbonate on Uranium Sorption to Hydrous Ferric Oxide

Waite et al., Geochim Cosmo. Acta, 58, 5465-5478, 1994

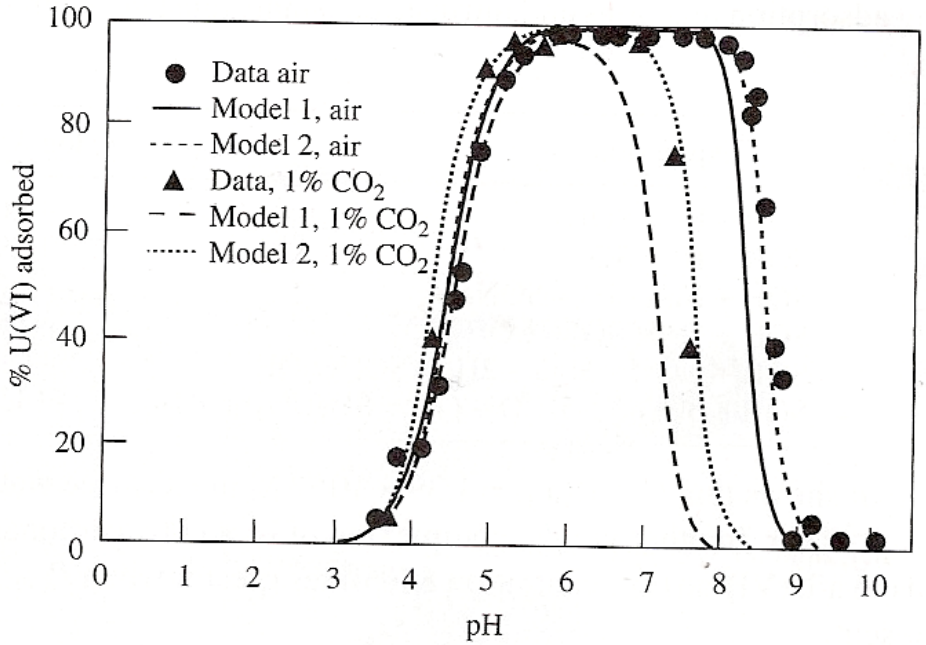

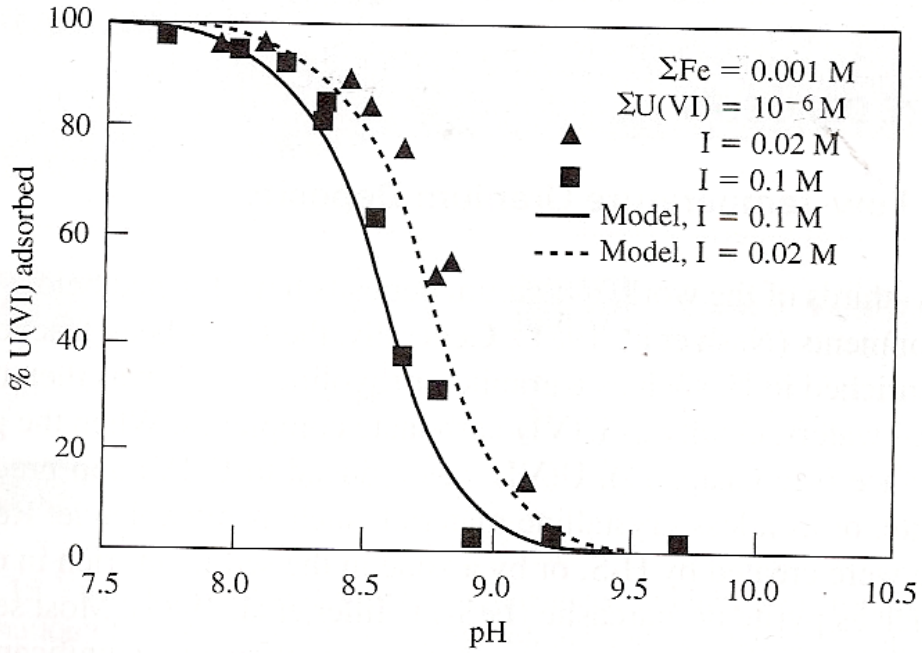

Effect of Carbonate on Uranium Sorption to Goethite

Hsi and Langmuir, Geochim Cosmochim. Acta, 49(11), 2423-2432, 1985

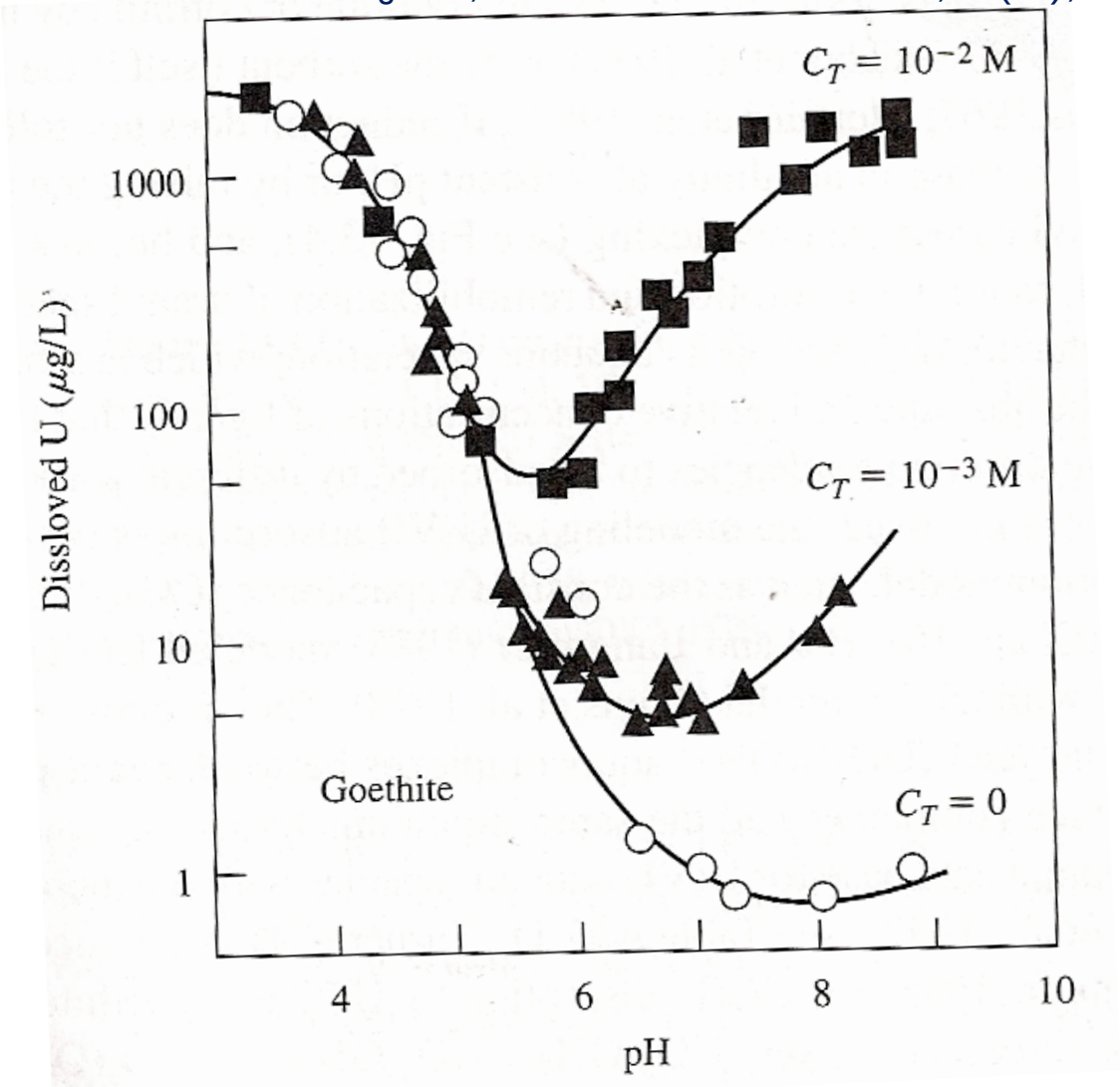

Uranium- Carbonate Ternary Complexes

Bargar et al., Geochimica et Cosmochimica Acta, 2000

- Ball and stick models of postulated uranium surface complexes
- All have the potential to facilitate uranium sorption

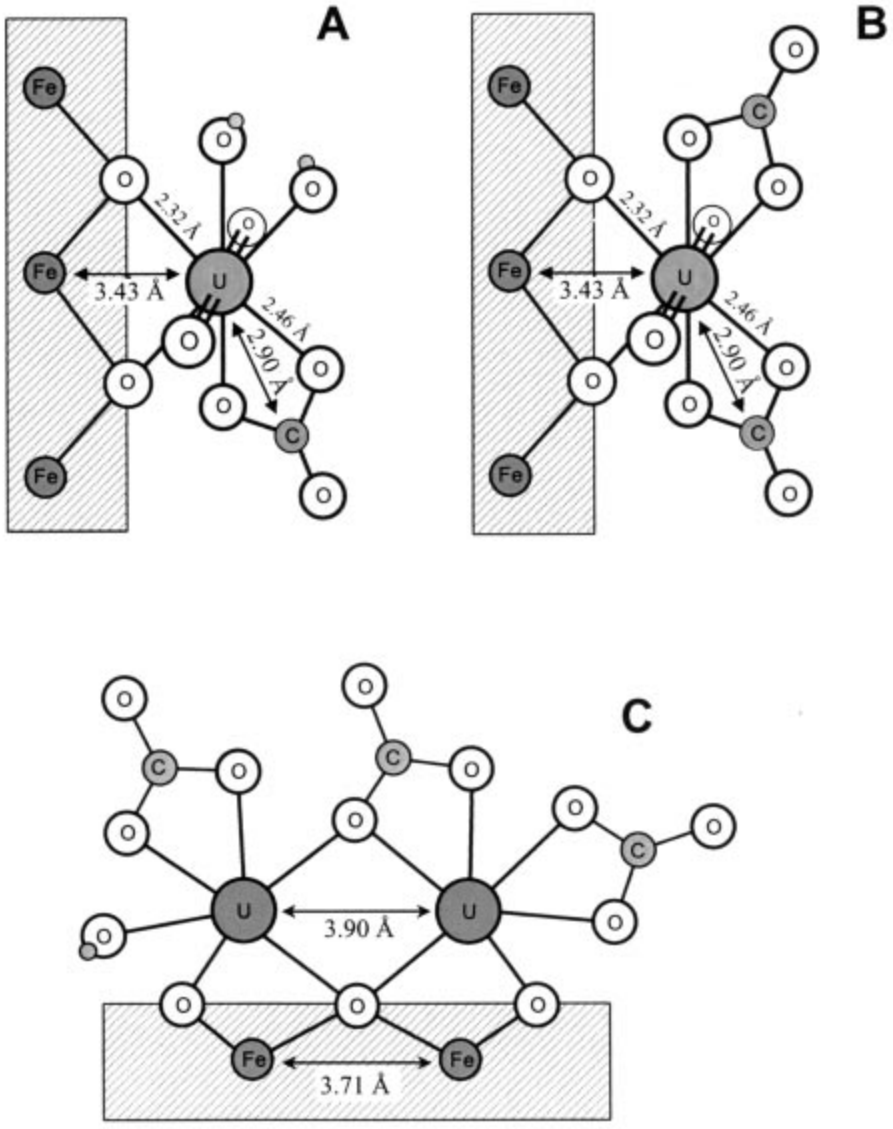

Determination of Ternary Surface-actinide-carbonate Species Arai et al., ES&T, 41, 3940-3944, 2007

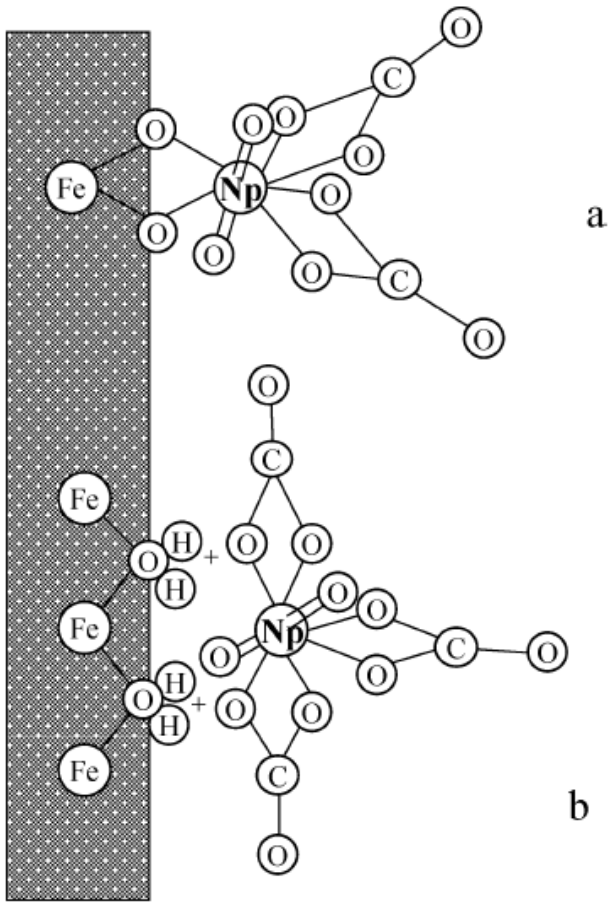

FIGURE 3. Ball-and-stick representation of Np(V) surface species on the iron octahedral structure of hematite based on the results of XAS analyses shown in Table 1. (a) Bis-carbonato−Np(V) inner-sphere ternary complex via bidentate mononuclear Np(V)−O_2−Fe linkage. (b) Tris-carbonato−Np(V) outer-sphere ternary complex.

In Situ Spectroscopic Evidence for Neptunium(V)-Carbonate Inner-Sphere and Outer-Sphere Ternary Surface Complexes on Hematite Surfaces

YUJI ARAI,*,† P. B. MORAN,‡,§ B. D. HONEYMAN,‡ AND J. A. DAVIS†

Department of Entomology, Soils and Plant Sciences, 270 Poole Agricultural Center, Clemson University, Clemson, South Carolina 29634-0315, Department of Environmental Science & Engineering, Colorado School of Mines, Coolbaugh Hall, Golden, Colorado 80401-1887, and Department of Chemistry and Geochemistry, Colorado School of Mines, Golden, 1500 Illinois Street, Golden, Colorado 80401

Np(V) surface speciation on hematite surfaces at pH 7−9 under $pCO_2 = 10^{-3.45}$ atm was investigated using X-ray absorption spectroscopy (XAS). In situ XAS analyses suggest that bis-carbonato inner-sphere and tris-carbonato outer-sphere ternary surface species coexist at the hematite−water interface at pH 7−8.8, and the fraction of outer-sphere species gradually increases from 27 to 54% with increasing pH from 7 to 8.8. The results suggest that the heretofore unknown Np(V)−carbonato ternary surface species may be important in predicting the fate and transport of Np(V) in the subsurface environment down gradient of high-level nuclear waste respositories.

Stabilization of U(V) surface complexes on mica

Ilton et al., Inorg. Chem. 2005

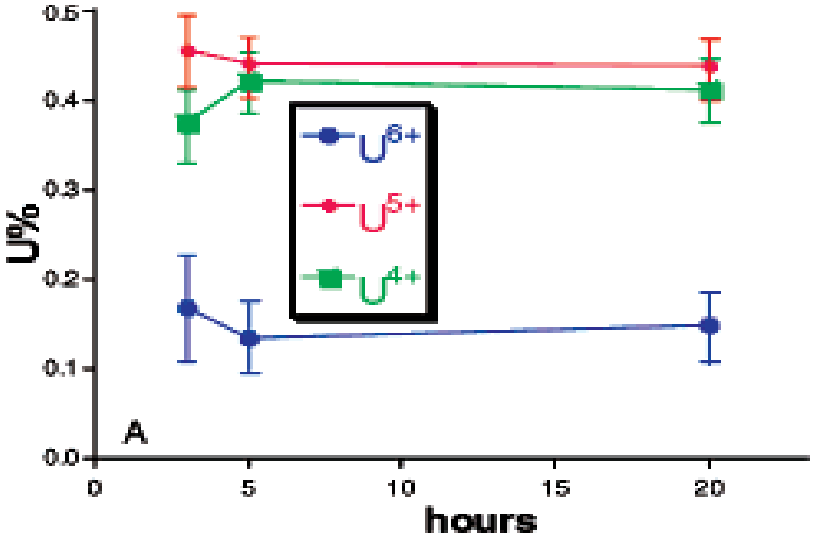

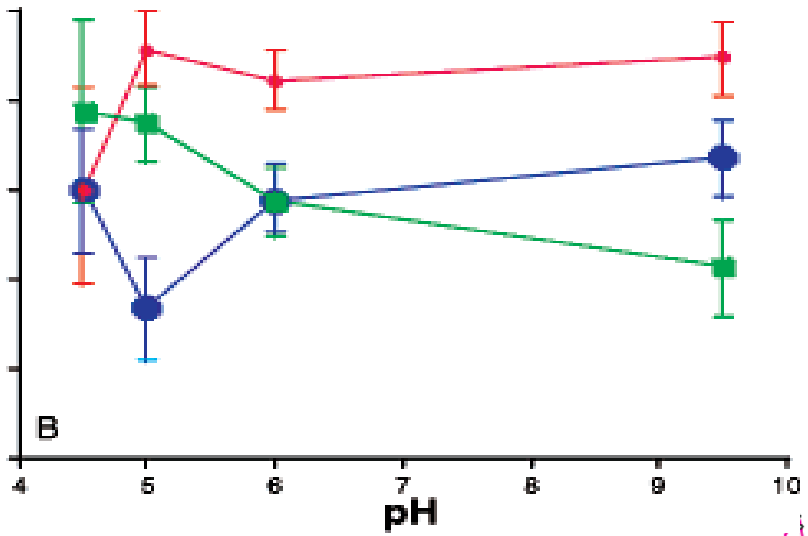

- Uranium oxidation state distribution as a function of time at pH 5 (left) and a function of pH after 3 hours (right)
- U(V) stabilized during reduction of U(VI) on ferrous mica surfaces

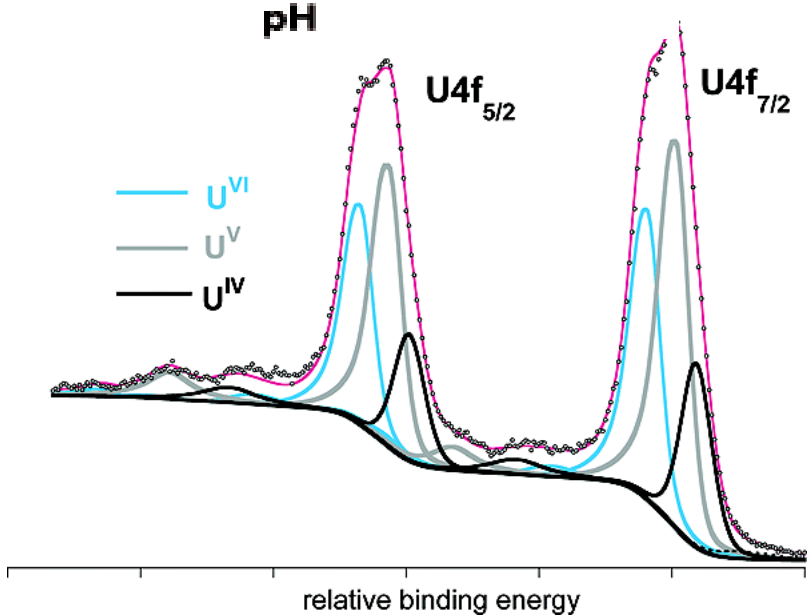

Influence of Humic Acid on Uranium Sorption Lenhart and Honeyman, 1999

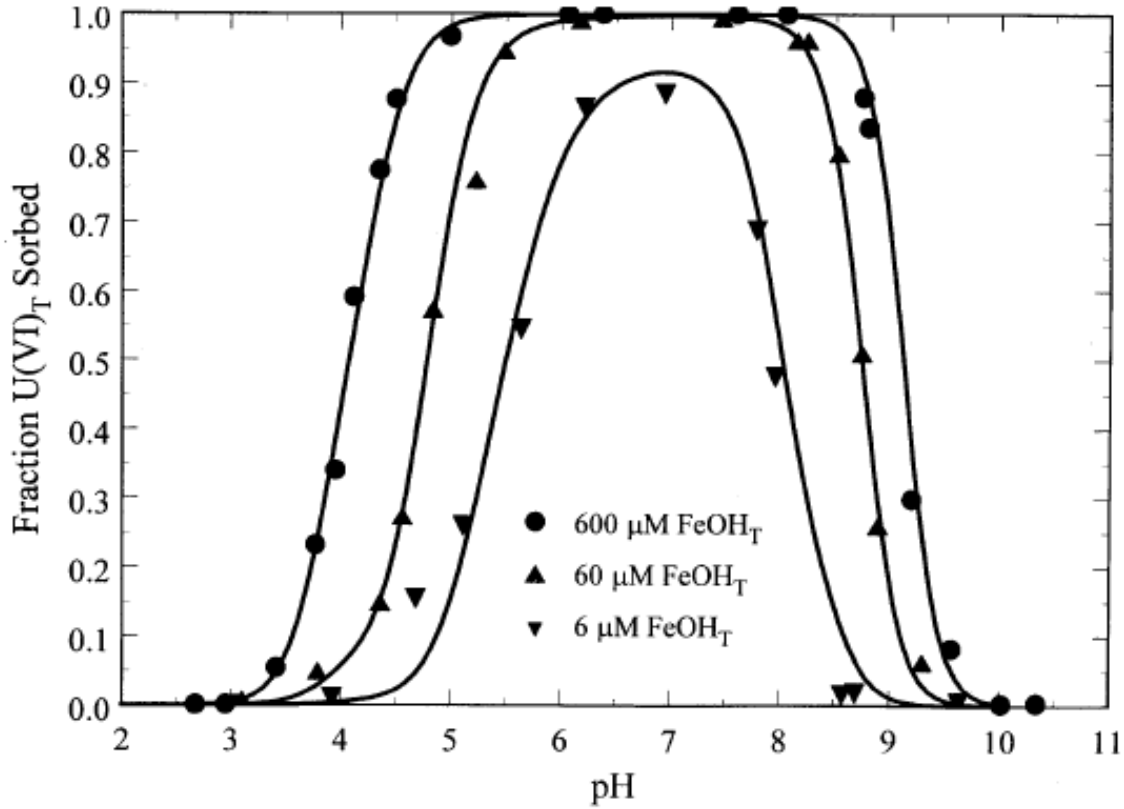

Fig. 2. Experimental results and FITEQL model simulations of fraction uranium sorbed onto 0.09 g/L, 0.9 g/L. and 9.0 g/L hematite at variable pH. Ionic strength = 0.1, $U(VI)_T = 10^{-6}$ M and atmospheric concentrations of CO_2. All material properties and model constants are in Tables 1, 2, and 3.

Influence of Humic Acid on Uranium Sorption Lenhart and Honeyman, 1999

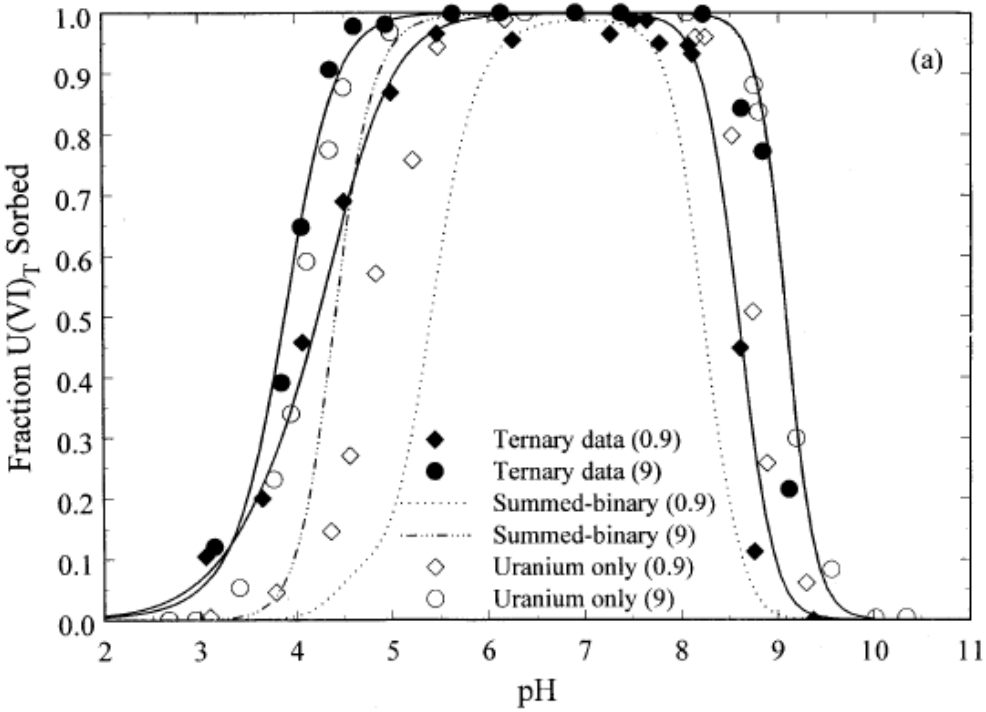

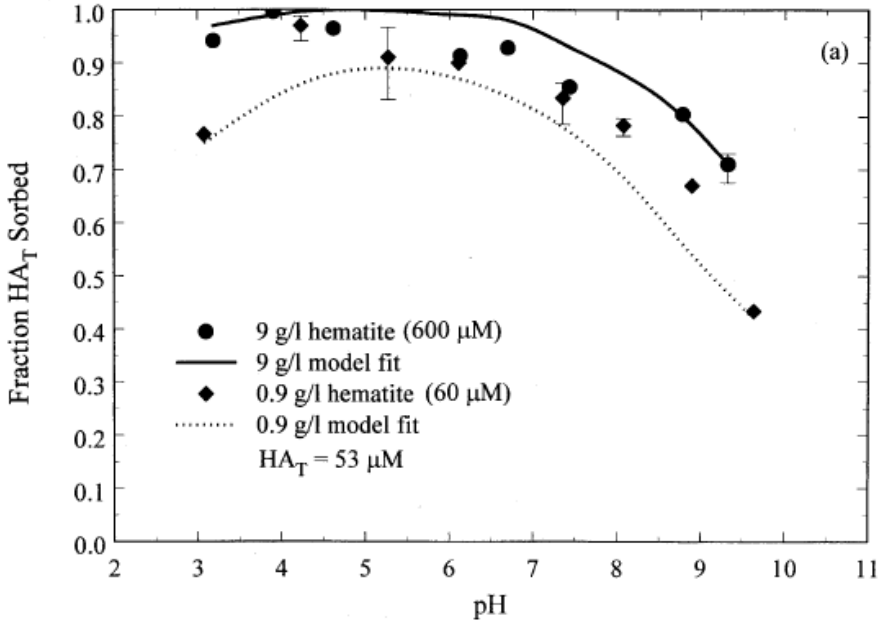

Influence of Humic Acid on Uranium Sorption Lenhart and Honeyman, 1999

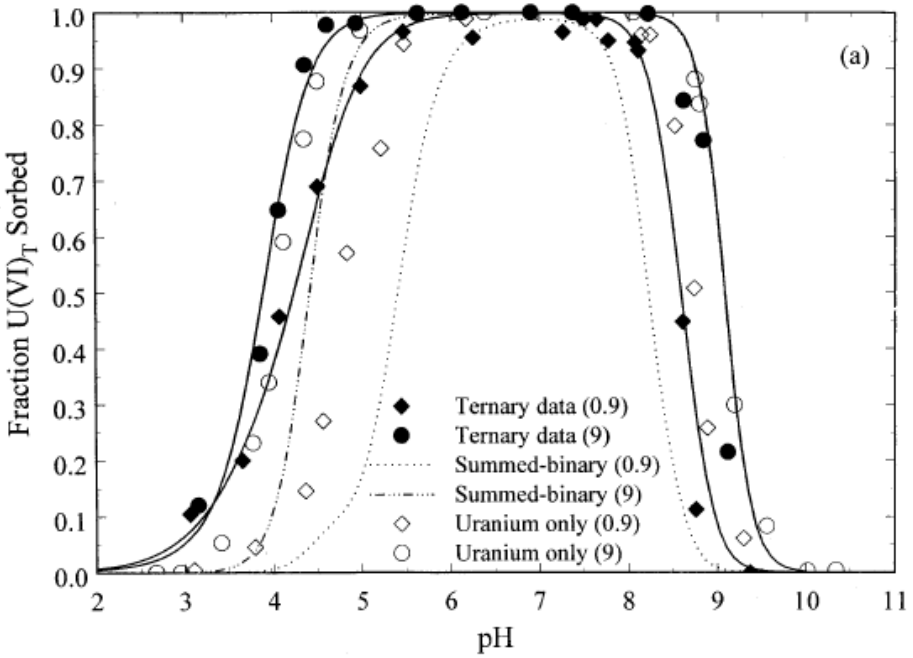

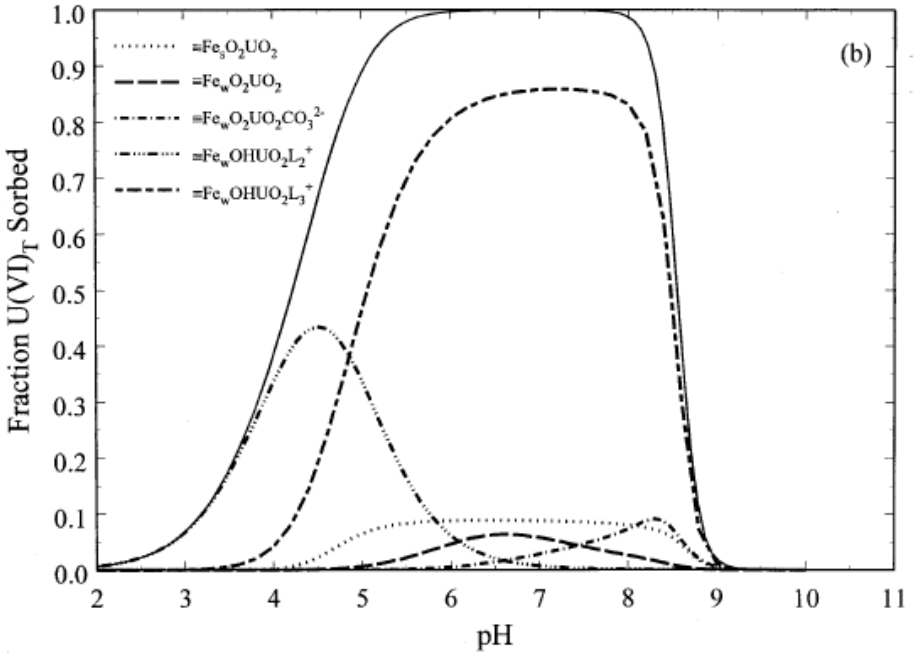

Precipitation/Dissolution

- Expected (nano)precipitates under environmental conditions

- See webinars on “Uranium Chemistry” and “Plutonium Chemistry” for detailed discussions of many solid phases

Uranium Bearing Solids

- Hundreds of known solid phases
- See Burns (1999) and Finch and Murakami (1999) for detailed discussions
- Insoluble phases primarily U(IV) phases as oxides, silicates and phosphates
  - $UO_2(c) + H_4SiO_4 \Leftrightarrow USiO_4(c) + 2H_2O$
- U(VI) minerals commonly formed via oxidation and weathering of U(IV) phases (examples below)

U(IV) Phase	U(VI) Phase
Uraninite, $UO_2(s)$	Autinite $Ca_2(UO_2)_2(PO_4)_2$
Coffinite, $USiO_4(s)$	Schoepite, $UO_3 \cdot 2.25H_2O$
	Cartonite, $K_2(UO_2)_2(VO_4)_2$

Relevant U(VI) Mineral Phases

from Sowder, Ph.D. Dissertation, Clemson University, 1999

Table IV. U(VI) minerals and phases.

FAMILY/phase	Structural Formula
UOHs	
schoepite	$[(UO_2)_8O_2(OH)_{12}]\cdot 12H_2O$ or $UO_3\cdot 2.25H_2O$
meta-schoepite	$[(UO_2)_8O_2(OH)_{12}]\cdot 10H_2O$ or $UO_3\cdot 2H_2O$
dehydrated schoepite	$[(UO_2)O_{0.25}(OH)_{1.5}]$ or $UO_3\cdot 0.75H_2O$
METAL UOHs	
becquerelite	$Ca[(UO_2)_6O_4(OH)_6]\cdot 8H_2O$
billietite	$Ba[(UO_2)_6O_4(OH)_6]\cdot 8H_2O$
compreignacite	$K_2[(UO_2)_6O_4(OH)_6]\cdot 8H_2O$
URANYL SILICATES	
soddyite	$(UO_2)_2(SiO_4)\cdot 2H_2O$
uranophane	$Ca(H_3O)_2[(UO_2)(SiO_4)]_2\cdot 3H_2O$
URANYL PHOSPHATES	
autunite	$Ca[(UO_2)_2(PO_4)_2]\cdot 8\text{-}12H_2O$
meta-autunite (I)	$Ca[(UO_2)_2(PO_4)_2]\cdot 6H_2O$
meta-autunite (II)	$Ca[(UO_2)_2(PO_4)_2]\cdot 4\text{-}6H_2O$
chernikovite	$H_2[(UO_2)_2(PO_4)_2]\cdot 8H_2O$ or $[(UO_2)H(PO_4)]\cdot 4H_2O$
uranyl orthophosphate	$(UO_2)_3(PO_4)_2\cdot 4H_2O$

Sequestration of U(VI) Via Sorption and Uranyl Phosphate Precipitation Fuller et al., 2002

Text from Fuller et al., Figure 6 Caption

- a) Backscatter SEM image of HA with 4700 ppm sorbed U(VI) (UHA-2C). U not detected by backscatter imaging or by EDS.
- (b) Backscatter image of HA with 77 500 ppm sorbed U(VI) (UHA-80K). Bright areas indicate secondary U phase. Only U and P were detected in this material by EDS.
- (c) Secondary electron image of autunite formed by reaction of U(VI) with HA at U:P) 1 (UHA-9) illustrating fine-grained precipitate and altered HA grains. The inset is higher magnification of an altered HA grain.
- (d) Secondary electron image of chernikovite precipitated in the absence of HA (U-P200).

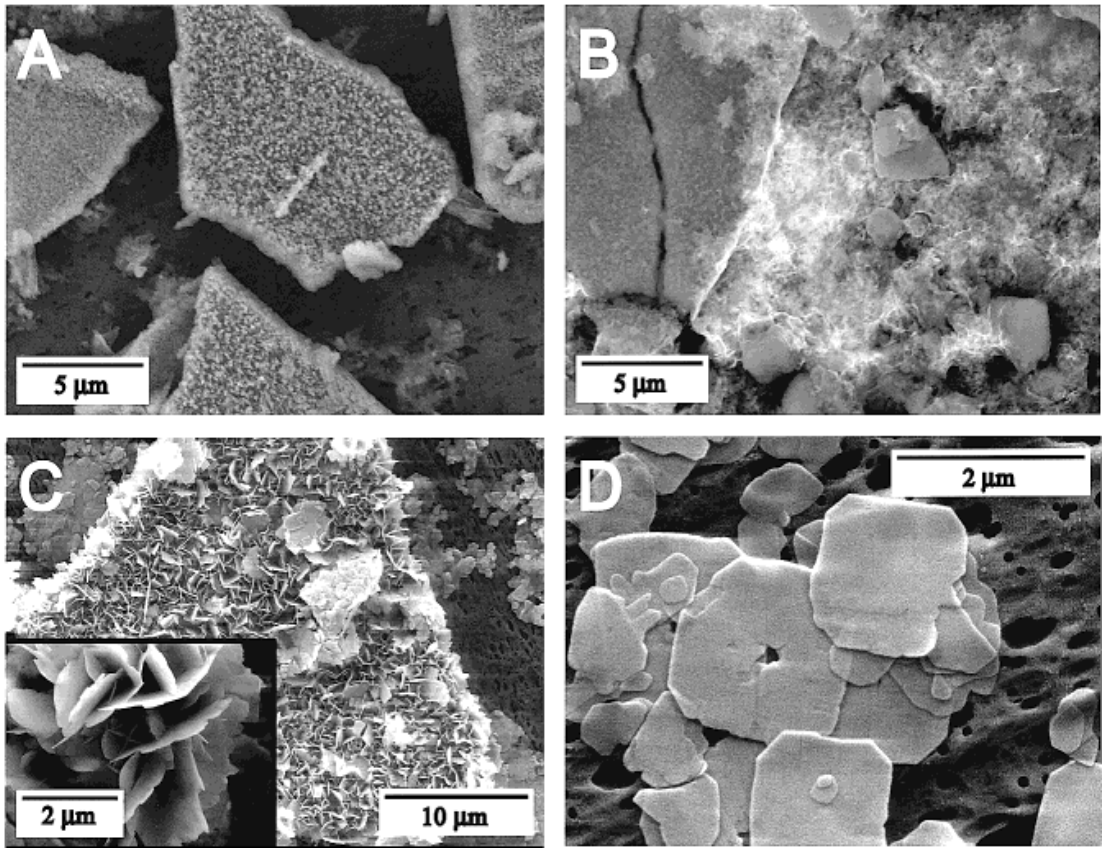

Case Study: Uranium Bioremediation

- A common approach to remediation of contaminated sites is to reduce mobile U(VI) to an insoluble/immobile U(IV) state
- Commonly achieved by stimulating microbial activity to promote reducing conditions
- Evidence for direct and indirect reduction of uranium
- Some indications that reoxidation of uranium may occur (Wan et al., 2005)

Influences of Microrganisms on Actinide Environmental Behavior Neu et al., 2010

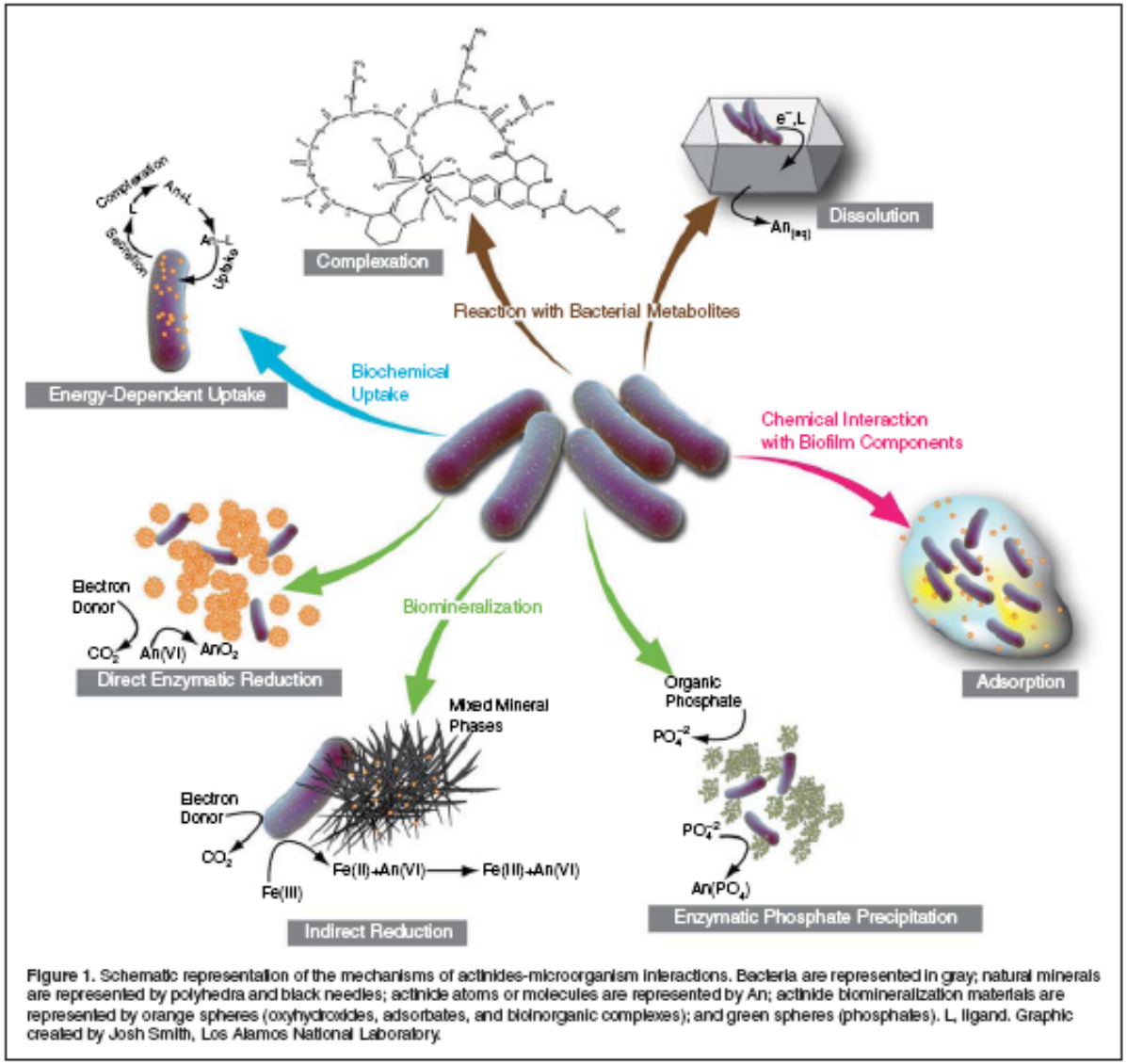

Figure 1. Schematic representation of the mechanisms of actinides-microorganism interactions. Bacteria are represented in gray; natural minerals are represented by polyhedra and black needles; actinide atoms or molecules are represented by An; actinide biomineralization materials are represented by orange spheres (oxyhydroxides, adsorbates, and bioinorganic complexes); and green spheres (phosphates). L, ligand. Graphic created by Josh Smith, Los Alamos National Laboratory.

Biogenic Uranium Nanoparticles

Burgos et al., Geochimica et Cosmochimica Acta 72 (2008) 4901–4915
Schofield et al., Environmental Science and Technology, 2008, 42, 7898-7904

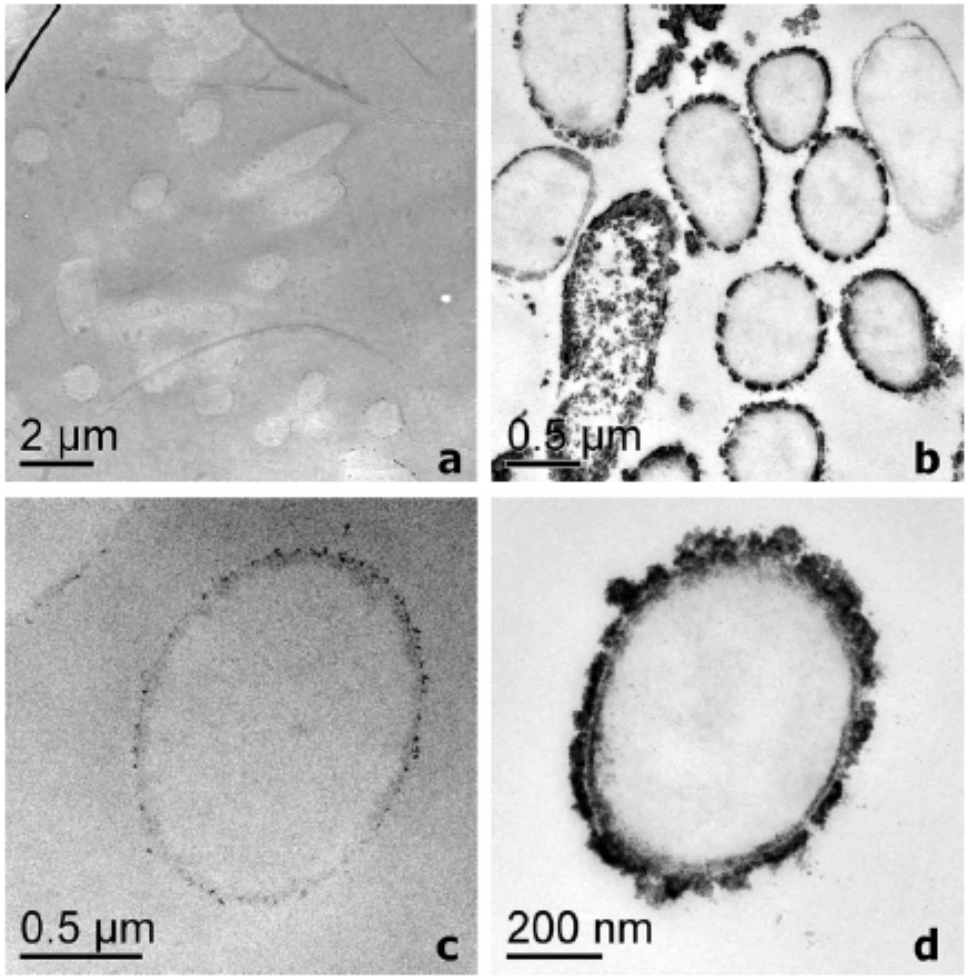

Burgos et al., 2008

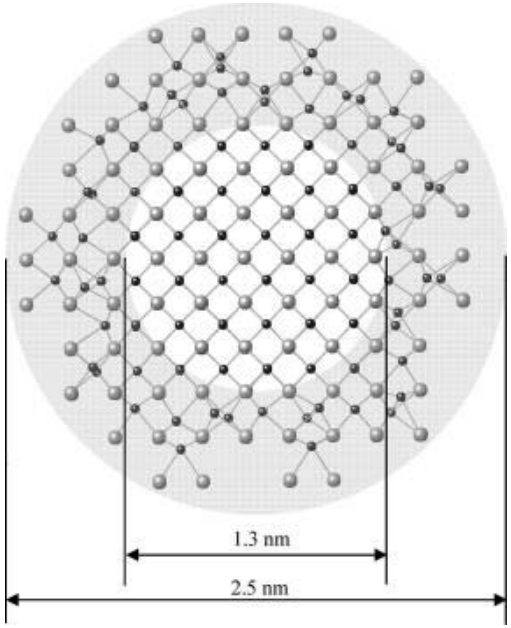

Schofield et al., 2008

U(VI) Reduction to Mononuclear U(IV)

Fletcher et al., Environ Sci. Tech., 2011

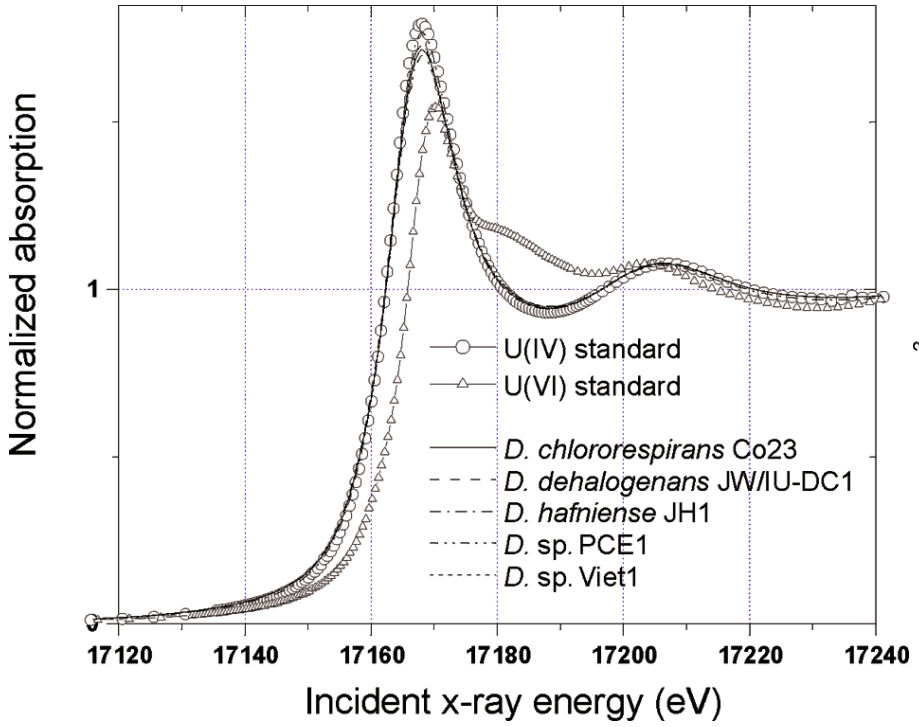

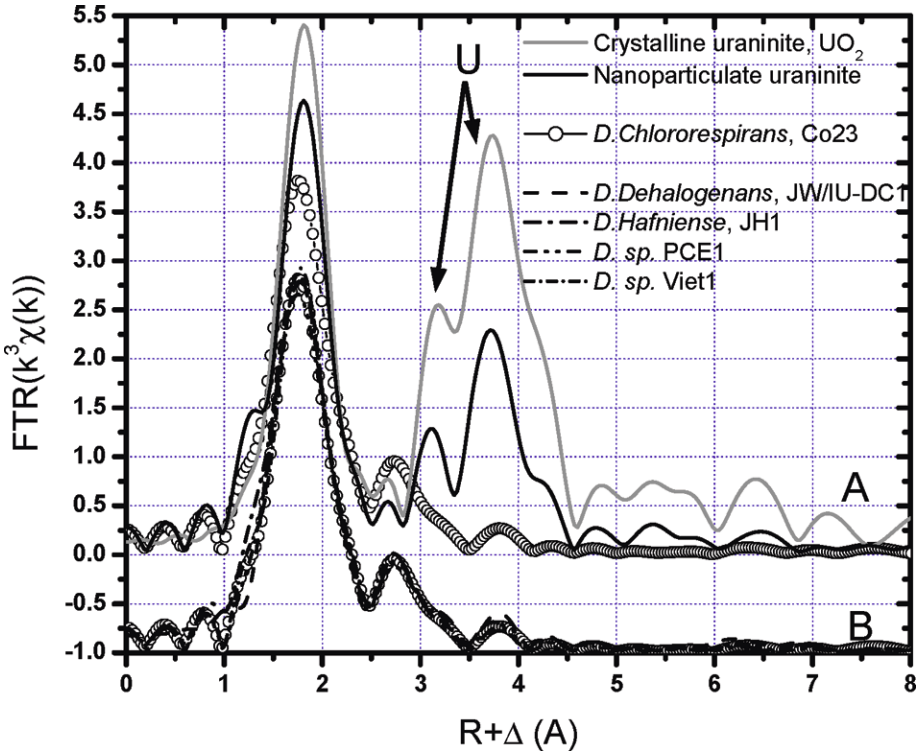

- Despite frequent observations of uraninite formation, mononuclear U(IV) was observed
- Bernier-Latmani et al., 2010, also observed several non-uraninite reduced species, which were primarily influenced by phosphorous metabolites

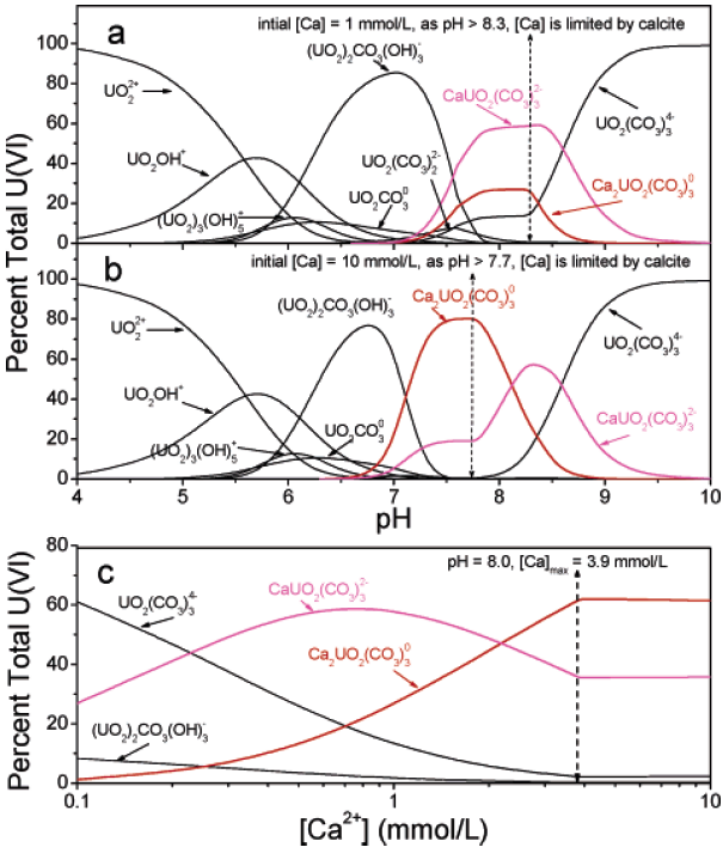

FIGURE 3. Aqueous U(VI) speciation distribution as a function of pH in the absence and presence of Ca^{2+} at [U(VI)] = 1 μmol/L, I = 0.1 mol/L $NaNO_3$, $P_{CO_2} = 10^{-3.5}$ atm, and 25 °C: (a) [Ca^{2+}] = 1 mmol/L, and (b) [Ca^{2+}] = 10 mmol/L. The formation constants of $CaUO_2(CO_3)_3^{2-}$ and $Ca_2UO_2(CO_3)_3^0$ are from this work and the others from (*15*). (c) Aqueous U(VI) speciation distribution as a function of [Ca^{2+}] at pH 8.0, [U(VI)] = 1 μmol/L, I = 0.1 mol/L $NaNO_3$, $P_{CO_2} = 10^{-3.5}$ atm, and 25 °C. As indicated the maximum aqueous calcium concentration is calculated to be 3.9 mmol/L at pH 8.0 with respect to calcite solubility.

Dong and Brooks, ES&T, 2006

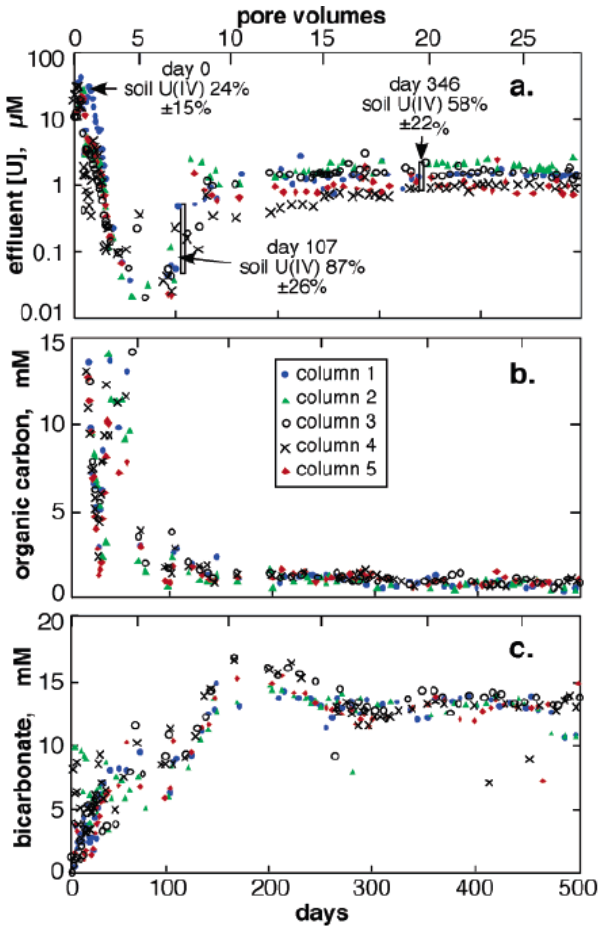

FIGURE 1. U, OC, and bicarbonate concentrations (all relative uncertainties < 10%) from five representative sediment columns. (a) Effluent U concentration trends show declines completed at ~day 60, increases began at ~day 100, and reached steady state at ~day 200. Bars indicate times for μ-XANES measurements of U oxidation states in sediments. (b) OC trends show 97% of injected lactate was being consumed, leaving 1 mM OC in effluents. (c) Bicarbonate trends show this major product of microbial respiration increased to 15 mM, then decreased to 13 mM after about day 215 because of switching to a lower flow rate (lower rate of OC supply).

Wan et al., ES&T, 2005

Field research sites

- Note there is a wealth of information on uranium remediation at DOE Integrated Field Research Sites
- These sites are managed within the Subsurface Biogeochemical Research program of the DOE Biological and Environmental Research, Climate and Environmental Sciences Program
- http://doesbr.org/research/ifrc.shtml
  - Hanford, WA: http://ifchanford.pnnl.gov/
  - Rifle, CO: http://ifcrifle.pnnl.gov/
  - Oak Ridge, TN: http://www.esd.ornl.gov/orifrc/

Summary

- Uranium exhibits remarkably complex behavior under environmental conditions
- Hundreds of known solid phases of varying chemistries
- Predominantly U(IV) and U(VI) states although U(III) and U(V) are accessible under environmental conditions
- Aqueous chemistry of U(VI) is profoundly influenced by carbonate complexation, including alkaline earth-uranium-carbonate ternary complexes
- Remediation strategies
  - Reduction of soluble and mobile U(VI) to insoluble and relatively immobile U(IV) is a common remediation strategy
  - Precipitation of insoluble U(VI) phosphate phases
- Numerous products observed during remediation activities, all of which have somewhat unique characteristics to the system in which they are formed

References

- Arai, Y., Moran, P.B., Honeyman, B.D., Davis, J.A., 2007. In situ spectroscopic evidence for neptunium(V)-carbonate inner-sphere and outer-sphere ternary surface complexes on hematite surfaces. Environmental Science & Technology, 41(11): 3940-3944.
- Brooks, S.C. et al., 2003. Inhihition of bacterial U(VI) reduction by calcium. Environmental Science & Technology, 37(9): 1850-1858.
- Burgos, W.D. et al., 2008. Characterization of uraninite nanoparticles produced by Shewanella oneidensis MR-1. Geochimica Et Cosmochimica Acta, 72(20): 4901-4915.
- Burns, P.C., 1999. The Crystal Chemistry of Uranium. Reviews in Mineralogy, 38: 23-90.
- Choppin, G.R., Rao, L.F., 1984. Complexation of Pentavalent and Hexavalent Actinides by Fluoride. Radiochimica Acta, 37(3): 143-146.
- Choppin, G.R., Wong, P.J., 1998. The chemistry of actinide behavior in marine systems. Aquatic Geochemistry, 4(1): 77-101.

References

- Clark, D.L., Hobart, D.E., Neu, M.P., 197272727295. Actinide Carbonate Complexes and Their Importance in Actinide Environmental Chemistry. Chemical Reviews, 95(1): 25-48.
- Dong, W.M., Brooks, S.C., 2008. Formation of aqueous MgUO2(CO3)(3)(2-) complex and uranium anion exchange mechanism onto an exchange resin. Environmental Science & Technology, 42(6): 1979-1983.
- Finch RJ, Murakami T (1999) Systematics and paragenesis of uranium minerals. In: Burns PC, Ewing RC (eds) Uranium: Mineralogy, Geochemistry and the Environment. Rev Mineral 38: 521-622.
- Hsi, C.K.D., Langmuir, D., 1985. Adsorption of Uranyl onto Ferric Oxyhydroxides - Application of the Surface Complexation Site-Binding Model. Geochimica Et Cosmochimica Acta, 49(9): 1931-1941.
- Kelly, S. D., Kemner, K. M., Brooks, S. C., 2007. X-ray absorption spectroscopy identifies calcium-uranyl-carbonate complexes at environmental concentrations. Geochimica et Cosmochimica Acta, 71: 821-834.
- Neu, M.P., Boukhalfa, H., Merroun, M.L., 2010. Biomineralization and biotransformations of actinide materials. Mrs Bulletin, 35(11): 849-857.

References

- Schofield, E.J. et al., 2008. Structure of Biogenic Uraninite Produced by Shewanella oneidensis Strain MR-1. Environmental Science & Technology, 42(21): 7898-7904.
- Shcherbina, N.S. et al., 2007. Redox and complexation interactions of neptunium(V) with quinonoid-enriched humic derivatives. Environmental Science & Technology, 41(20): 7010-7015.
- Silva, R.J., Nitsche, H., 1995. Actinide environmental chemistry. Radiochimica Acta, 70-1: 377-396.
- Sposito, G., 1989. The Chemistry of Soils, The Chemistry of Soils.
- Stumm, W., 1992. Chemistry of the Solid-Water Interface: Processes at the Mineral-Water and Particle-Water Interface in Natural Systems. Wiley Press, Chicago, 428 pp.
- Vallet, V., Wahlgren, U., Schimmelpfennig, B., Szabo, Z., Grenthe, I., 2001. The mechanism for water exchange in UO2(H2O)(5) (2+) and UO2(oxalate)(2)(H2O) (2-), as studied by quantum chemical methods. Journal of the American Chemical Society, 123(48): 11999-12008.

References

- Waite, T.D., Davis, J.A., Payne, T.E., Waychunas, G.A., Xu, N., 1994. Uranium(Vi) Adsorption to Ferrihydrite - Application of a Surface Complexation Model. Geochimica Et Cosmochimica Acta, 58(24): 5465-5478.
- Wan, J.M. et al., 2005. Reoxidation of bioreduced uranium under reducing conditions. Environmental Science & Technology, 39(16): 6162-6169.
- Wang, Z. et al., 2008. A spectroscopic study of the effect of ligand complexation on the reduction of uranium(VI) by anthraquinone-2,6-disulfonate (AH(2)DS). Radiochimica Acta, 96(9-11): 599-605.

Future NAMP Radiochemistry Webinars

- Actinide Chemistry Series
  - Analytical Chemistry of Uranium and Plutonium
  - Source Preparation for Alpha Spectroscopy
  - Sample Dissolution
- Radium Chemistry

NAMP website: www.inl.gov/namp